

The cortical protein Lte1 promotes mitotic exit by inhibiting the spindle position checkpoint kinase Kin4

Daniela Trinca Bertazzi, Bahtiyar Kurtulmus, and Gislene Pereira

DKFZ-ZMBH Alliance, German Cancer Research Center, 69120 Heidelberg, Germany

The spindle position checkpoint (SPOC) is an essential surveillance mechanism that allows mitotic exit only when the spindle is correctly oriented along the cell axis. Key SPOC components are the kinase Kin4 and the Bub2–Bfa1 GAP complex that inhibit the mitotic exit-promoting GTPase Tem1. During an unperturbed cell cycle, Kin4 associates with the mother spindle pole body (mSPB), whereas Bub2–Bfa1 is at the daughter SPB (dSPB). When the spindle is mispositioned, Bub2–Bfa1 and Kin4 bind to both SPBs, which enables Kin4 to phosphorylate Bfa1

and thereby block mitotic exit. Here, we show that the daughter cell protein Lte1 physically interacts with Kin4 and inhibits Kin4 kinase activity. Specifically, Lte1 binds to catalytically active Kin4 and promotes Kin4 hyperphosphorylation, which restricts Kin4 binding to the mSPB. This Lte1-mediated exclusion of Kin4 from the dSPB is essential for proper mitotic exit of cells with a correctly aligned spindle. Therefore, Lte1 promotes mitotic exit by inhibiting Kin4 activity at the dSPB.

Introduction

The unequal distribution of cell fate determinants during asymmetric cell division is a fundamental process that underlies the generation of cell diversity in a variety of multicellular organisms (Yamashita et al., 2007). The positioning of the mitotic spindle relative to the cell polarity axis is critical to mediate asymmetric cell divisions (Siller and Doe, 2009).

Several mechanisms ensure correct spindle alignment in the asymmetrically dividing unicellular organism, budding yeast *Saccharomyces cerevisiae*. First, spindle positioning relative to the intrinsic polarity axis of the cell is ensured by two partially redundant pathways; one reliant upon the function of the conserved protein Kar9, the other upon the microtubule motor protein dynein (Segal and Bloom, 2001). Second, if spindle orientation fails, a surveillance mechanism called the spindle positioning checkpoint (SPOC) pauses cell cycle progression until proper spindle alignment is achieved (Fraschini et al., 2008; Caydası et al., 2010a).

Under normal cell cycle progression, the mitotic exit network (MEN) initiates mitotic exit and cytokinesis in late anaphase. The MEN is a GTPase-driven signaling pathway whose components associate with the yeast microtubule organizing

center, the spindle pole body (SPB). MEN signaling starts with the activation of the GTPase Tem1 that triggers the sequential activation of the protein kinase Cdc15 and the Dbf2–Mob1 kinase complex. Dbf2–Mob1 promotes the full activation of the protein phosphatase Cdc14, which is needed to promote Cdk inactivation, leading to mitotic exit and cytokinesis (Bardin and Amon, 2001). Feedback mechanisms involving Cdc14 and Cdk contribute to MEN activation at the level of Cdc15 and Dbf2–Mob1 (Jaspersen and Morgan, 2000; König et al., 2010). However, the mechanisms by which the activation of Tem1 is controlled remain debatable. Tem1 preferentially associates with the SPB that enters the daughter cell (dSPB; Bardin et al., 2000; Pereira et al., 2000). Based on genetic studies and the presence of the guanine nucleotide exchange factor (GEF) homology domain, the putative GEF Lte1 has been implicated in Tem1 activation (Keng et al., 1994; Shirayama et al., 1994b). Lte1 is confined at the daughter cell cortex and the entrance of the dSPB bound to Tem1 brings Tem1 in close proximity to Lte1, thus promoting Tem1 activation (Bardin et al., 2000; Pereira et al., 2000). However, Lte1 is not essential for mitotic exit at temperatures above 30°C and no GEF activity toward Tem1 has been

Correspondence to Gislene Pereira: g.pereira@dkfz.de

Abbreviations used in this paper: GAP, GTPase-activating protein; GEF, guanine nucleotide exchange factor; MEN, mitotic exit network; SPB, spindle pole body; SPOC, spindle position checkpoint.

© 2011 Bertazzi et al. This article is distributed under the terms of an Attribution-Noncommercial-Share Alike-No Mirror Sites license for the first six months after the publication date (see <http://www.rupress.org/terms>). After six months it is available under a Creative Commons License (Attribution-Noncommercial-Share Alike 3.0 Unported license, as described at <http://creativecommons.org/licenses/by-nc-sa/3.0/>).

detected with purified proteins (Adames et al., 2001; Geymonat et al., 2009a).

During an unperturbed cell cycle the bipartite GTPase-activating protein (GAP) complex, Bub2–Bfa1, maintains Tem1 in an inactive state until Bfa1 is inactivated through phosphorylation by the polo-like kinase Cdc5. In late mitosis, this phosphorylation decreases Bub2–Bfa1 GAP activity, promoting mitotic exit (Hu et al., 2001; Geymonat et al., 2003). If the spindle becomes misaligned, the SPOC kinase Kin4 phosphorylates Bfa1, blocking the ability of Cdc5 to inactivate Bfa1 (D'Aquino et al., 2005; Pereira and Schiebel, 2005; Maekawa et al., 2007; Caydas and Pereira, 2009).

Both Kin4's localization and kinase activity are important for its control of Bub2–Bfa1 function. The catalytic activity of Kin4 is regulated by the bud neck–associated kinase Elm1. Elm1 phosphorylates a conserved threonine residue in the conserved activation loop (T-loop) of Kin4 (Caydas et al., 2010b; Moore et al., 2010). However, activation of Kin4 by Elm1 is not sufficient to provide SPOC function. Another prerequisite is Kin4 localization to the mother cell cortex and SPBs. Kin4 SPB and cortex association are regulated by the activity of the phosphatase PP2A subunit Rts1 via an unknown mechanism (Chan and Amon, 2009; Caydas et al., 2010b).

Whereas deletion of *KIN4* has only minor consequences upon mitotic progression under normal growth conditions, excessive production of Kin4 transcripts from artificial promoters blocks cell cycle progression in late anaphase in a Bub2–Bfa1-dependent manner (D'Aquino et al., 2005). Similarly, placing a mutated Kin4 variant within daughter cells also causes mitotic exit delays (Chan and Amon, 2010). Thus, it is tempting to speculate that Kin4 kinase activity must be kept high inside the mother cell to promote Kin4's function if the spindle is misoriented; on the other hand, Kin4 kinase activity must be kept low within the daughter cell to allow mitotic exit. The inhibitory mechanisms that restrain Kin4 kinase activity locally are unknown. Here, we established that Lte1 physically interacts with the catalytically active form of Kin4. *In vivo* studies showed that Lte1 acts as an inhibitor of Kin4 catalytic activity toward Bfa1. Furthermore, we established that Lte1 is necessary to promote Kin4 hyperphosphorylation and exclusion from the dSPB during anaphase. We therefore propose that Lte1 promotes mitotic exit by inhibiting the activity and dSPB localization of the MEN inhibitor Kin4.

Results

Kin4 and Lte1 physically interact in vivo and in vitro

To identify Kin4-interacting proteins, we purified Kin4 from yeast cell lysates using the tandem affinity purification (TAP) strategy (Puig et al., 2001). Mass spectrometric (MS) analysis of the composition of the Kin4–TAP complex identified the known Kin4 interactor, Bfa1, and components of the SPB (Fig. 1 A and Fig. S1 A; Pereira and Schiebel, 2005). In addition, we identified a large number of peptides corresponding to Lte1 in the Kin4–TAP complex (Fig. S1 A). Likewise, when we purified Lte1–TAP complexes we identified Kin4 alongside the known Lte1-interacting

proteins Kel1, Kel2, Ras1, and Ras2 (Fig. 1 A and Fig. S1 A; Höfken and Schiebel, 2002; Yoshida et al., 2003). Co-purification of Lte1 and Kin4 was unexpected because Kin4 preferentially localizes at the mother cell cortex, whereas Lte1 is mostly associated with the cortex of the bud (Bardin et al., 2000; Pereira et al., 2000; D'Aquino et al., 2005; Pereira and Schiebel, 2005).

To confirm the physical association between Kin4 and Lte1, we performed immunoprecipitation experiments using functional hemagglutinin (HA) and Myc-tagged fusion proteins. Kin4-9Myc coprecipitated with Lte1-6HA in HA specific pull-downs (Fig. 1 B) and, vice-versa (Fig. S1 B). We considered the possibility that the interaction between Kin4 and Lte1 arose from copurification of large subfragments of the cell cortex. However, this was not the case, as neither Kin4-6HA coprecipitated with a plasma membrane protein of the daughter cell, Ist2-3Myc (Fig. S1 C) (Takizawa et al., 2000), nor did Lte1-6HA coprecipitate the mother cortex–associated protein, Sfk1-9Myc (Fig. S1 D) (Audhya and Emr, 2002). We thus conclude that Lte1 and Kin4 are companions found within common complexes.

Additionally, Kel1 peptides were also found in the Kin4 purification and a fraction of Kin4-6HA coimmunoprecipitated with Kel1-9Myc (Fig. 1 C). This interaction was specific for Kel1, as Kin4 did not coimmunoprecipitate with the closely related molecule Kel2 or the Lte1 interactors Ras1 and Ras2 (Fig. S1, A and E; and unpublished data). To better characterize Lte1–Kin4–Kel1 interactions, we asked whether the absence of any one component would influence the association between the others. The association of Lte1 with Kin4 was unaffected by loss of Kel1 (Fig. 1 D), whereas deletion of *LTE1* impaired binding of Kel1 to Kin4 (Fig. 1 E). This suggests that Lte1 bridges the interaction between Kel1 and Kin4.

We next asked whether Lte1 directly interacts with Kin4. Here, we used purified, recombinant Lte1 and Kin4 proteins. In contrast to full-length Lte1, N- and C-terminal truncated Lte1 constructs were soluble and could be purified from *Escherichia coli* cells (Fig. 1, F and G). Both 6His-Lte1-N and 6His-Lte1-C proteins bound GST-Kin4 but neither bound GST alone (Fig. 1, F and G; lanes 8–11). We therefore concluded that Lte1 and Kin4 are present in common complexes *in vivo* and physically associate *in vitro*.

Misplacement of Lte1 but not Kel1 to the mother cell cortex promotes mitotic exit of cells with misaligned spindle

We next asked how *KEL1* and *LTE1* are functionally linked to *KIN4*. Overexpression of *KIN4* is toxic (D'Aquino et al., 2005). We found that co-overexpression of *LTE1*, but not of *KEL1*, rescued the toxicity of Kin4 overproduction (Fig. 2 A), suggesting a functional interplay between Lte1 and Kin4 but not Kel1 and Kin4 *in vivo*.

Overexpression of *LTE1*, expression of a mutant variant of *LTE1* that accumulates in the mother cell cortex, or disruption of the mother–daughter cell diffusion barrier (defective bud neck) causes SPOC deficiency in cells with misaligned spindles (Bardin et al., 2000; Castillon et al., 2003; Geymonat et al., 2009a). To test whether misplacement of Kel1 would impair SPOC function in a similar manner to Lte1, we established a strategy that

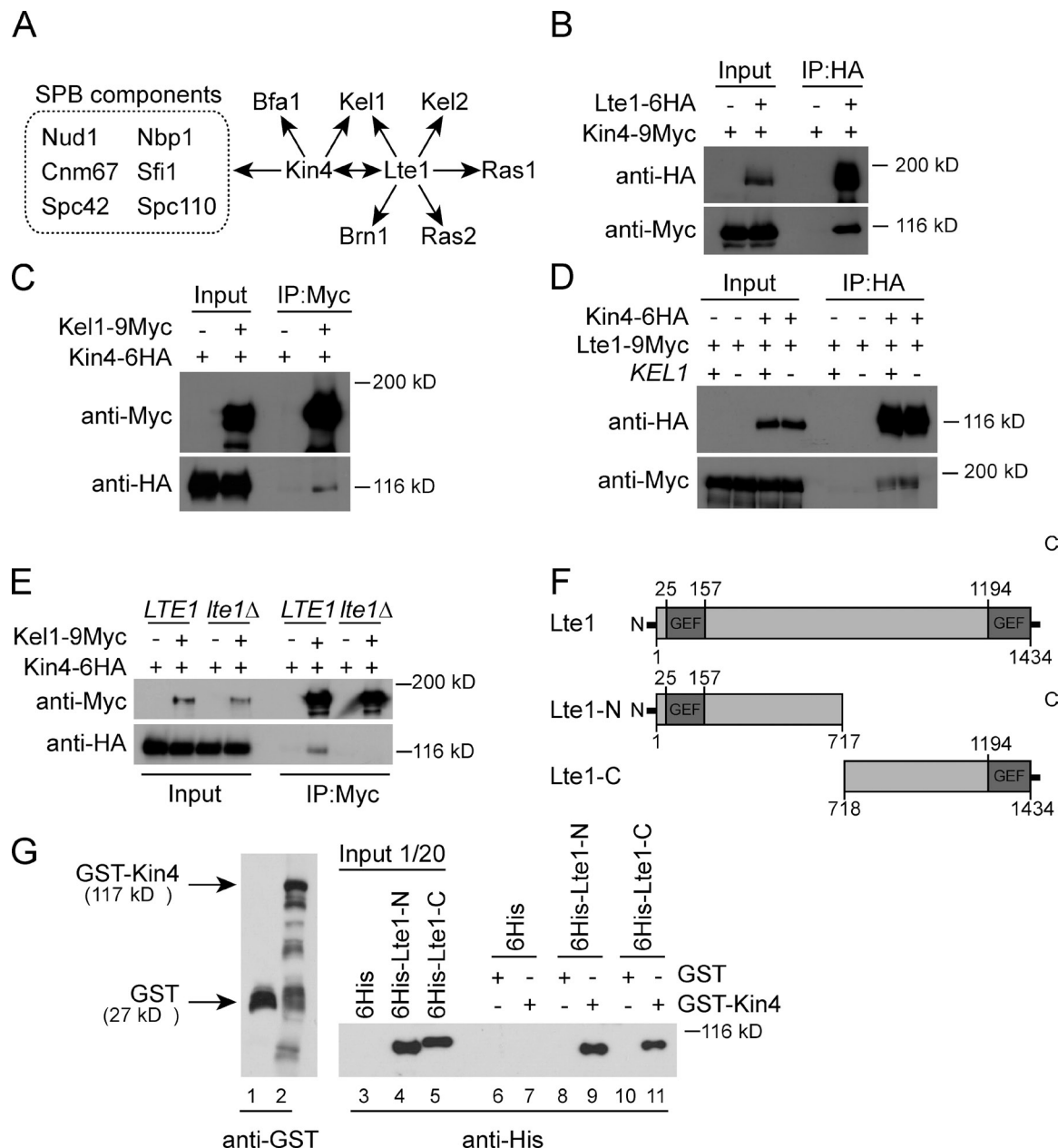
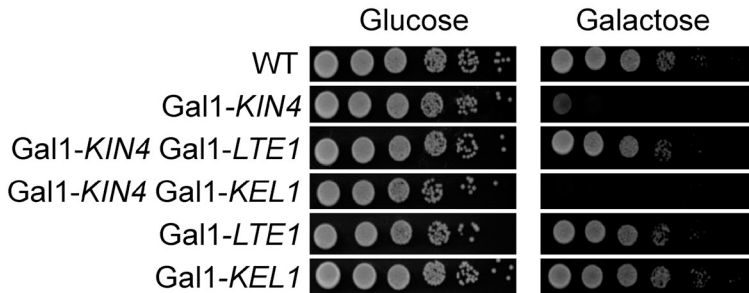


Figure 1. Lte1 interacts with Kin4 in vitro and in vivo. (A) Kin4- and Lte1-interacting partners found by MS analysis. (B–E) Kin4 interacts with Lte1 and Kel1. Immunoprecipitations using anti-HA or anti-Myc beads as indicated. (F and G) In vitro binding assay using bacterially expressed *KIN4* and *LTE1*. (F) Lte1 truncations used in G; numbers represent amino acid positions. (G) Immunoblotting of bacterially expressed GST (lane 1) and GST-Kin4 (lane 2) bound to glutathione-Sepharose beads. Protein extracts of *E. coli* expressing 6His (lane 3), 6His-Lte1-N (lane 4), and 6His-Lte1-C (lane 5) were incubated with GST (lanes 6, 8, and 10) or GST-Kin4 (lanes 7, 9, and 11) for 2 h at 4°C.

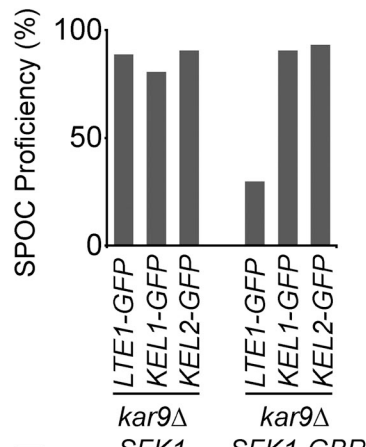
could easily be transferred to a variety of GFP-tagged proteins expressed under the control of the endogenous promoter. For this, we adopted the GFP entrapment strategy based on the GFP-binding protein (GBP), which efficiently binds to GFP and GFP-tagged proteins when expressed in human cells (Rothbauer et al., 2008). This approach was successful in budding yeast because we were able to constitutively target bud neck and nuclear associated GFP-tagged proteins to SPBs of cells expressing the SPB component *SPC42* fused to GBP (unpublished data). To enrich Lte1 and Kel1 in the mother cell compartment, we expressed Lte1-GFP and Kel1-GFP in strains carrying the mother cell cortex protein Sfk1 tagged with GBP (Sfk1-GBP; Fig. 2, B–E).

Fusion of Sfk1 with GBP altered neither cell cycle progression nor SPOC proficiency of *kar9* Δ cells (Fig. 2 B; unpublished data). Lte1-GFP and Kel1-GFP were efficiently enriched in the mother cell cortex in *SFK1-GBP kar9* Δ strains, irrespective of spindle alignment (Fig. 2, C and D). Confinement of Lte1-GFP to the mother cell cortex by this GBP entrapment strategy decreased the SPOC proficiency in *SFK1-GBP kar9* Δ cells that had misaligned spindles (Fig. 2, B and C), in agreement with previous reports (D'Aquino et al., 2005; Geymonat et al., 2009a). In contrast to Lte1-GFP, mislocalization of Kel1-GFP to the mother cell cortex did not alter SPOC function (Fig. 2, B and D). Also Kel2-GFP that associated with Lte1, yet did not

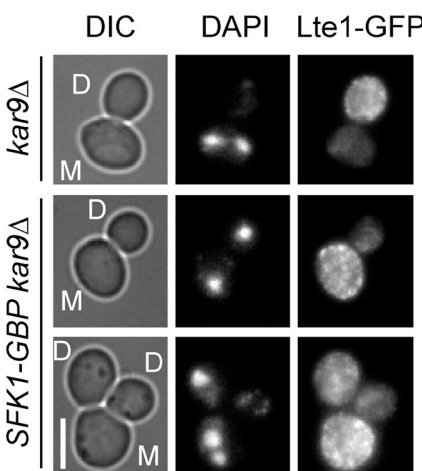
A



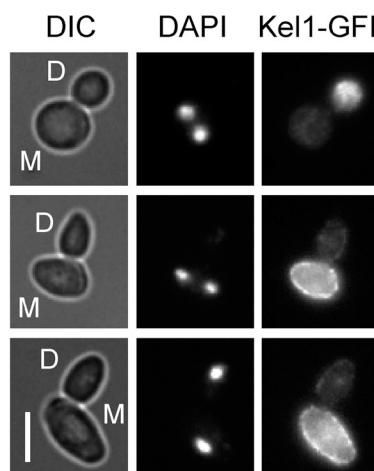
B



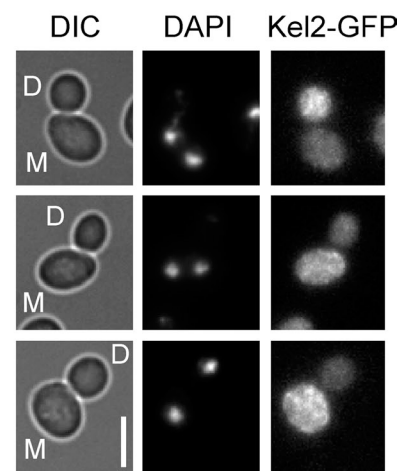
C



D



E



F

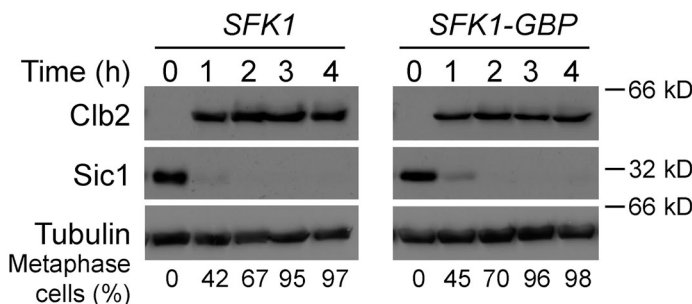


Figure 2. Lte1 inhibits Kin4 function toward Bfa1 in vivo. (A) Co-overexpression of *LTE1* rescues the lethality arising from *Gal1-KIN4* overexpression. Serial dilutions of cells spotted on YPAR plates containing either glucose or galactose to inhibit or induce the expression of Gal1 promoter, respectively. (B) SPOC proficiency in the indicated strains grown at 23°C and shifted to 30°C for 4 h before inspection. One representative experiment of three is shown. (C–E) *kar9Δ* or *SFK1-GBP kar9Δ* cells expressing *LTE1-GFP* (C), *KEL1-GFP* (D), and *KEL2-GFP* (E) were analyzed by fluorescence microscopy after incubation for 4 h at 30°C. Mother (M) and daughter (D) cell bodies are indicated. Cells in anaphase with correctly aligned or misoriented spindles are shown. The cell with two buds in *SFK1-GBP kar9Δ LTE1-GFP* is indicative of inappropriate mitotic exit. DNA was DAPI stained. Bars, 5 μ m. (F) *SFK1* and *SFK1-GBP* cells carrying *LTE1-GFP* were arrested with α -factor and released into nocodazole-containing media. Clb2 and Sic1 levels were determined by immunoblotting at the indicated time points. Tubulin served as a loading control.

form a complex with Kin4 (Fig. S1), had no inhibitory effect on SPOC in *SFK1-GBP kar9Δ* cells (Fig. 2, B and E). Thus Lte1, but neither Kel1 nor Kel2, bypassed the SPOC once improperly located in the mother cell compartment.

Moreover, mother cortex-located Lte1 did not impair the metaphase arrest induced by treatment of cells with the microtubule-depolymerizing drug, nocodazole (Fig. 2 F). In contrast to

the late anaphase arrest induced by SPOC, which requires both Tem1 inhibition and Kin4 function (D'Aquino et al., 2005; Pereira and Schiebel, 2005), nocodazole-induced metaphase arrest does not require Kin4; however, it can be bypassed by Tem1 activation (Chan and Amon, 2009). Thus, it is most likely that mother cell-enriched Lte1 promotes mitotic exit of cells with misaligned spindles by inhibiting Kin4 rather than activating Tem1.

Interaction between Kin4 and Lte1 requires active Kin4

To investigate the requirements for the Kin4-Lte1 interaction in vivo, we asked whether the binding of Kin4 to Lte1 was restricted to a particular phase in the cell cycle. We found Kin4 and Lte1 interacting in all phases of the cell cycle and in cells where the SPOC was active (Fig. S2, A and B). This may indicate that a fraction of Lte1 and Kin4 interacts throughout the cell cycle, although the majority of both proteins were kept in different compartments.

Using our GBP strategy, we found that bringing Lte1 to the mother cell cortex led to a 30–40% increase in the amount of Lte1 interacting with Kin4 in immunoprecipitations (Fig. S2 C), supporting the idea that Kin4–Lte1 complexes might be facilitated if Lte1 and Kin4 were present in the same subcellular compartment. We therefore pursued the idea that Kin4 and Lte1 may, to some extent, colocalize in the cytoplasm during the entire cell cycle. Indeed, inspection of live cells coexpressing functional *KIN4-GFP LTE1-3Cherry* (Maeder et al., 2007) revealed that although Lte1 and Kin4 accumulated most strongly in the daughter and mother cell bodies, respectively, they were not entirely excluded from the opposite cellular compartments (Fig. 3 A). Interestingly, just after cytokinesis, Kin4 remained associated with the bud neck and the new bud, in which Lte1 accumulated (Fig. 3 A). At the time that Kin4 accumulated at the bud neck, Lte1 was more evenly dispersed (Fig. 3 A). These data suggested that a fraction of Lte1 and Kin4 may indeed associate with one another throughout the cell cycle.

Importantly, Lte1 was unable to bind to the kinase-dead Kin4-T209A and to two other catalytic inactive Kin4 mutants (Fig. 3 B and Fig. S2 D). The interaction between Kin4 and Lte1 was also drastically reduced in *elm1Δ* cells, in which Kin4 is catalytically inactive (Caydasi et al., 2010b; Moore et al., 2010). The absence of Lte1–Kin4 complexes was not directly related to SPOC deficiency, as Lte1 still associated with Kin4 in *rts1Δ* cells, which are SPOC deficient with Kin4 catalytic activity similar to wild-type cells (Fig. 3 C; Chan and Amon, 2009; Caydasi et al., 2010b). Furthermore, overexpression of *LTE1-3Cherry*, using the inducible Gal1 promoter, caused a strong accumulation of Kin4-GFP but not Kin4-T209A-GFP (both expressed endogenously) in the bud (Fig. 3 D), further supporting the notion that the catalytic activity of Kin4 is required for its association with Lte1.

Lte1 inhibits the kinase activity of Kin4 in vitro

To understand the functional relevance of the Kin4–Lte1 interaction described here, we investigated whether Kin4 influenced the phosphorylation or localization of Lte1. When we compared *KIN4* wild-type cells with *kin4Δ* cells, we failed to detect any differences in either the phosphorylation or localization profiles of Lte1 with or without SPOC activation (unpublished data). Furthermore, purified Kin4 was not able to phosphorylate recombinant Lte1 in vitro (unpublished data). We therefore consider it unlikely that Kin4 phosphorylates Lte1 or influences its localization.

The fact that Lte1 physically associates with Kin4 prompted us to ask whether Lte1 regulates Kin4 catalytic activity. For this, Kin4 in vitro kinase activity toward Bfa1 was measured in the

presence of increasing levels of purified 6His-Lte1-N or 6His-Lte1-C (Fig. 4). 6His-GFP was used as a control to demonstrate that addition of buffer and an unrelated protein did not influence Kin4 kinase activity (Fig. 4 A, lanes 1 and 2). Purified GST-Kin4 but not the kinase-dead variant (GST-Kin4-T209A), enriched from yeast cell lysates, phosphorylated Bfa1 in vitro (Fig. 4 A, lanes 3 and 4). 6His-Lte1-N significantly inhibited the phosphorylation of Bfa1 by Kin4 in a dose-dependent manner (Fig. 4 B). An inhibition of ~64% in Kin4 specific activity was reached at the highest concentration of 6His-Lte1-N tested (Fig. 4 B). 6His-Lte1-C also inhibited Kin4 kinase activity, although not as efficiently as 6His-Lte1-N (Fig. 4 C; 34% inhibition). Thus, Lte1 inhibits Kin4 catalytic activity in vitro.

Lte1 is an inhibitor of Kin4 function in vivo

Kin4 is catalytically active during every cell cycle even when SPOC activation is not triggered (D'Aquino et al., 2005; Caydasi et al., 2010b). The fact that co-overexpression of *LTE1* and *KIN4* was not lethal for cell growth (Fig. 2 A), in contrast to *KIN4* overexpression alone (Fig. 2 A), supports the notion that cells must maintain a balance between Kin4 and Lte1 activities to achieve normal cell cycle progression. If true, one would expect cells lacking *LTE1* to be more sensitive to increasing amounts of Kin4 compared with wild-type cells. Indeed, although wild-type cells were able to grow with additional gene copies of *KIN4* supplied by either a centromeric (CEN-*KIN4*) or a 2μ-based plasmid (2μ-*KIN4*; Fig. 5 A), the addition of extra copies of *KIN4*, even from a centromeric plasmid, drastically impaired growth of *lte1Δ* cells (Fig. 5 A). Deletion of *BFA1* rescued this lethality (Fig. 5 A), showing that the toxicity of *KIN4* likely arose from an inhibition of the MEN via the Bub2–Bfa1 GAP complex. The accumulation of anaphase cells (indicative of a mitotic exit defect) in *lte1Δ* strains carrying an additional copy of CEN-*KIN4* confirmed this conclusion (unpublished data). In contrast, anaphase cells did not accumulate in *lte1Δ bfa1Δ* CEN-*KIN4* cells (unpublished data). Thus, Lte1 counterbalances Kin4 activity in a dose-dependent manner in vivo.

Considering that Lte1 inhibited Kin4 catalytic activity in vitro (Fig. 4), we reasoned that Kin4 catalytic activity should increase in the absence of *LTE1*. However, we did not observe any significant difference in the specific kinase activity of Kin4-6HA enriched from wild-type and *lte1Δ* cells from asynchronous cultures or from cultures whose cell cycle progression was arrested in G1-, S-, meta- and late anaphase or by SPOC activation (Fig. S3, A–C). Importantly, Lte1 was not present in the Kin4 immunoprecipitates used in the kinase assays, due to the stringent washing conditions required to eliminate cross-contaminating activity from other kinases (unpublished data).

To assess the role of Lte1 in the regulation of Kin4 kinase activity in vivo, we investigated the phosphorylation pattern of the established Kin4 substrate Bfa1 in the presence or absence of *LTE1*. Bfa1 becomes phosphorylated by the polo-like kinase Cdc5 at anaphase onset (Hu et al., 2001); this phosphorylation causes a transient appearance of the most hyperphosphorylated form of Bfa1-3HA (Fig. 5, B and C; asterisk). Kin4 activity counteracts this phosphorylation (D'Aquino et al., 2005; Pereira and

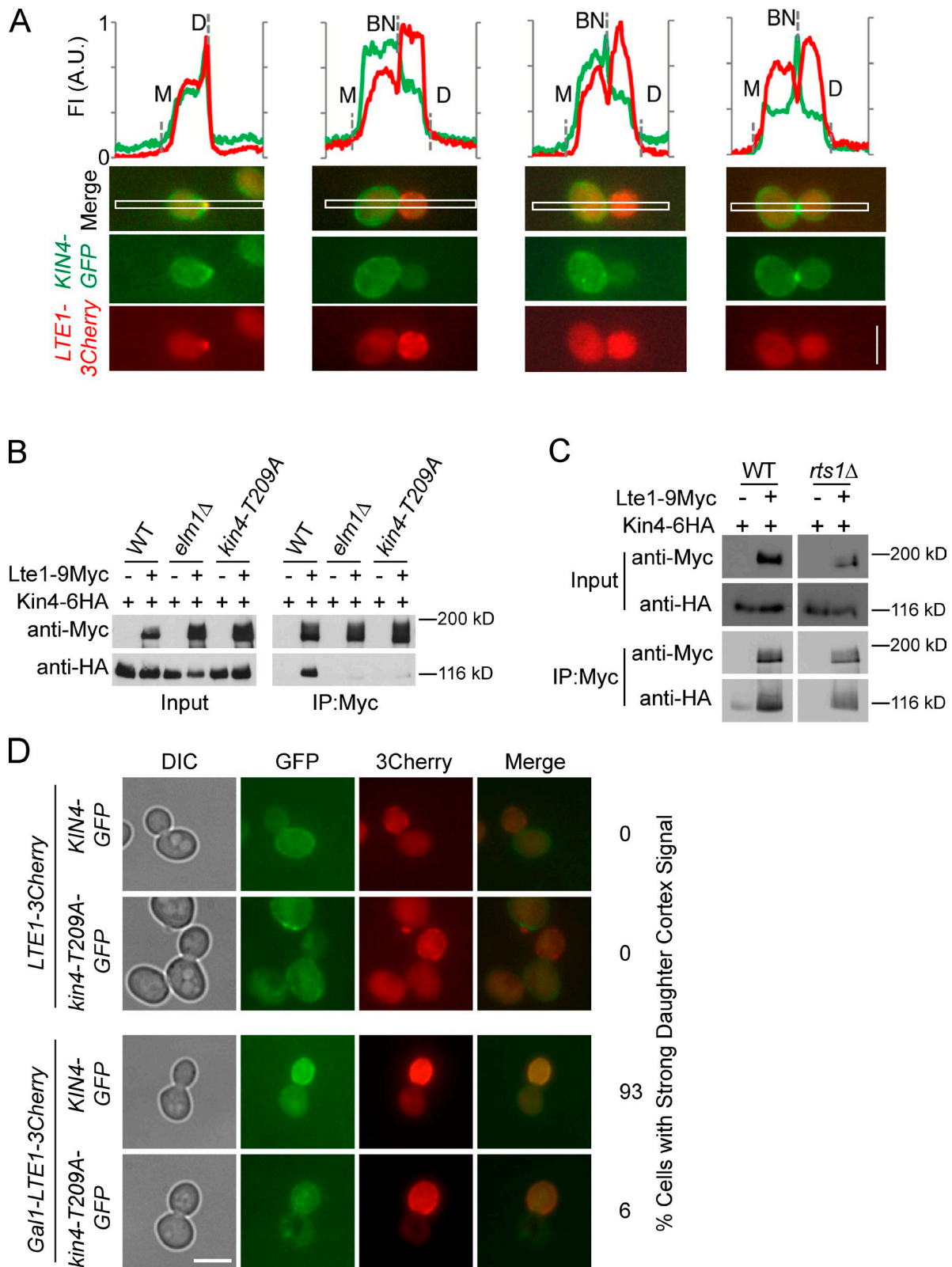


Figure 3. Kin4 catalytic kinase activity is required for Kin4-Lte1 interaction. (A) Representative frames and fluorescence intensity line traces of cells expressing *KIN4-GFP LTE1-3Cherry*. Line profiles above the images represent the fluorescence intensities (FI) in arbitrary units (A.U.), measured for the indicated rectangular area, for Kin4-GFP (green lines) and Lte1-3Cherry (red lines). Note that FI is not comparable between cells. Cell boundaries in each graph are indicated as M and D, and bud neck region as BN. Bar, 5 μ m. (B) *LTE1* and *LTE1-9Myc* strains carrying *KIN4-6HA* (WT), *KIN4-6HA elm1Δ*, and *KIN4-T209A-6HA* were subjected to immunoprecipitation using anti-Myc beads. (C) Interaction between *Lte1-9Myc* and *Kin4-6HA* was investigated in *RTS1* (WT, wild type) and *rtt1Δ* cells upon immunoprecipitation of *Lte1-9Myc* with anti-Myc beads. (D) Localization of *Kin4-GFP* and *Kin4-T209A-GFP* in strains carrying *LTE1-3Cherry* (no overexpression) and *Gal1-LTE1-3Cherry* (overexpression), growing in galactose-containing medium. Bars, 5 μ m.

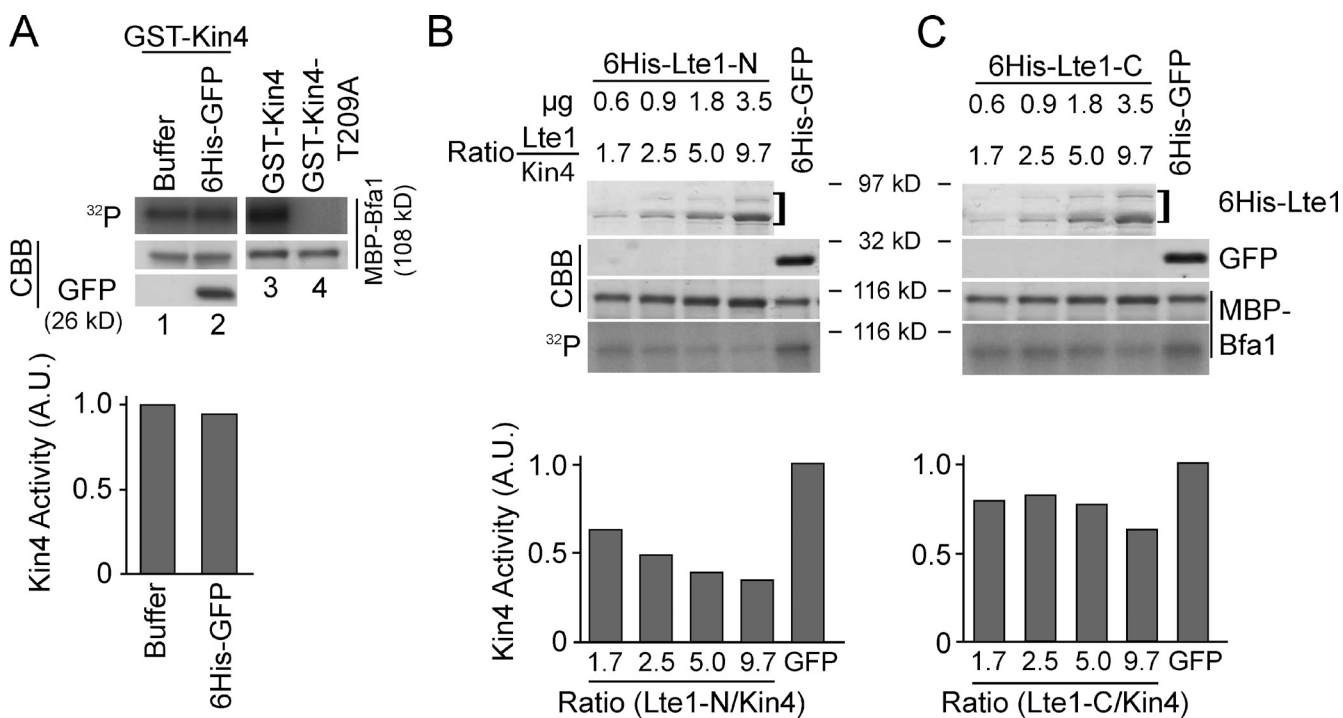


Figure 4. Lte1 inhibits the catalytic activity of Kin4 in vitro. (A) Yeast-purified GST-Kin4 or GST-Kin4-T209A were incubated with kinase buffer (lane 1) or purified 6His-GFP (lane 2) in the absence or presence of increasing amounts of 6His-Lte1-N (B) or 6His-Lte1-C (C) as indicated. Reactions were preincubated for 5 min at 30°C before adding MBP-Bfa1 and further incubating for 30 min at the same temperature. Autoradiographs (^{32}P), Coomassie-stained protein gels, and specific Kin4 kinase activity (in arbitrary units) are shown. Molar ratios were calculated based on protein molecular weight and concentration used in each reaction. One out of two experiments is shown.

Schiebel, 2005). Bfa1 hyperphosphorylation by Cdc5 was even more apparent in cells arrested in late anaphase by depletion of Tem1 (Fig. 5 B, asterisk). Strikingly, accumulation of Cdc5-derived hyperphosphorylated Bfa1-3HA was not observed in the absence of Lte1 (Fig. 5 B). Deletion of *KIN4* in Tem1-depleted *lte1* Δ cells restored Bfa1-3HA hyperphosphorylation (Fig. 5 B). This indicates that the lack of Bfa1 hyperphosphorylation in Tem1-depleted *lte1* Δ cells was not due to reduced Cdc5 kinase activity, *per se*. More likely it was caused by increased Kin4 activity. The inhibition of Bfa1 hyperphosphorylation, caused by lack of *LTE1*, was also observed during an unperturbed anaphase (Fig. 5 C and Fig. S4) or upon cell cycle release from nocodazole-induced metaphase block (Fig. S4). Importantly, deletion of *KIN4* in the *lte1* Δ background restored Bfa1 hyperphosphorylation in all aforementioned experiments (Fig. S4). However, because Bfa1 hyperphosphorylation was only partially restored in *lte1* Δ *kin4* Δ nocodazole-treated cells (Fig. S4 B), we cannot rule out the possibility that Lte1 might also control Bfa1 phosphorylation in a Kin4-independent manner. Together, the data show that Lte1 has a role upstream of Tem1 in the down-regulation of Kin4 activity toward Bfa1 during anaphase.

Lte1 promotes Kin4 hyperphosphorylation

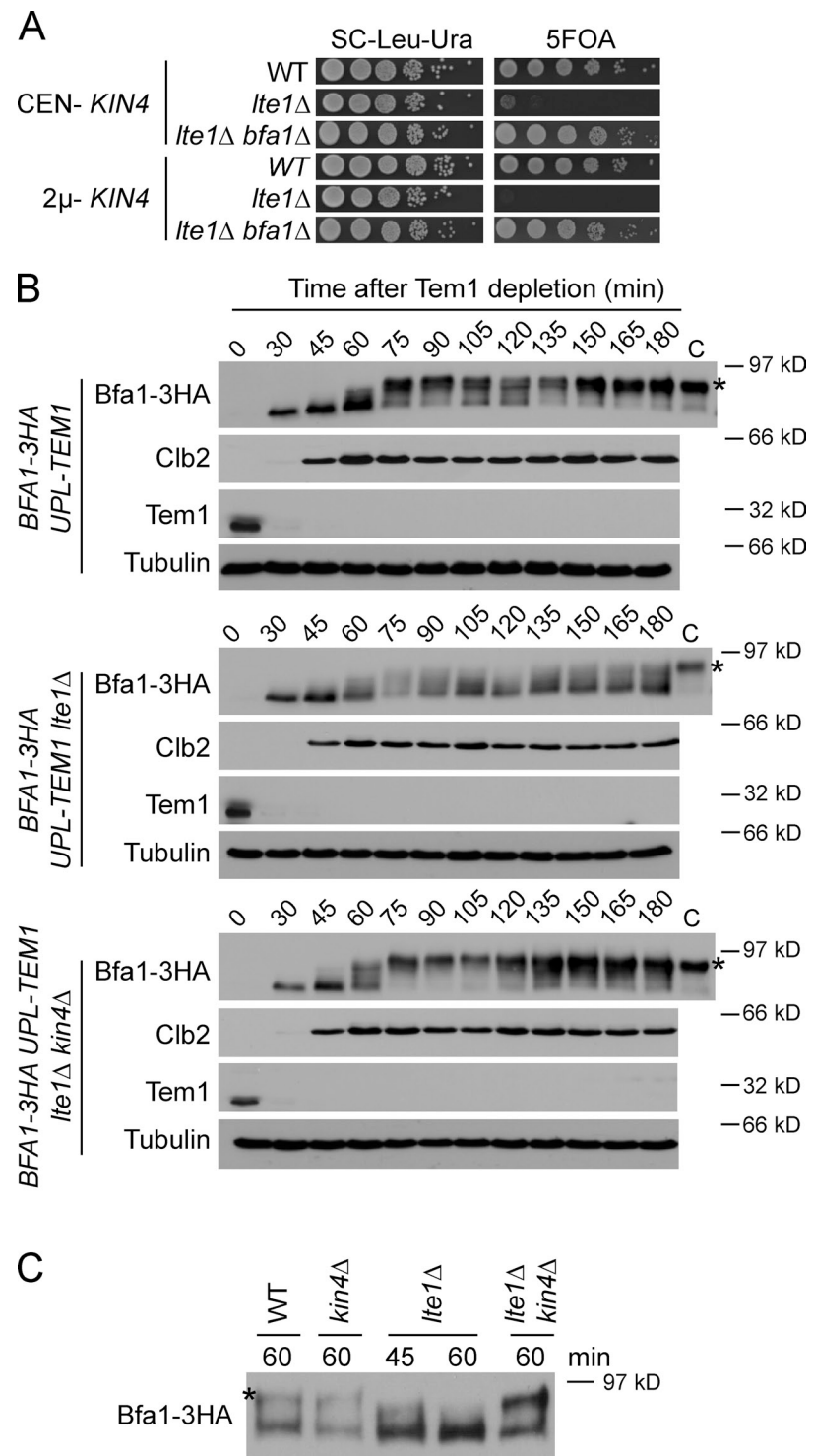
To explore the mechanisms by which Lte1 influences Kin4 phosphorylation *in vivo*, we asked whether Lte1 affected Kin4 phosphorylation and/or localization. Because Kin4 hyperphosphorylation increased upon SPOC activation (Chan and Amon, 2009; Caydası et al., 2010b), we analyzed Kin4-6HA in wild-type and *lte1* Δ cells that had been synchronized in G1 phase and subsequently

treated with nocodazole to activate the SPOC (Fig. 6 A). Slower migrating, hyperphosphorylated Kin4 forms were observed in wild-type but not in *lte1* Δ cells (Fig. 6 A, asterisk). The lack of Kin4 hyperphosphorylation in *lte1* Δ was even more apparent when nocodazole-treated cells reassumed cell cycle progression after nocodazole wash-out (Fig. 6 B). The effect of Lte1 upon Kin4 phosphorylation was not restricted to SPOC activation via nocodazole, as cells held in metaphase by depletion of the APC activator Cdc20 (Gal1-*CDC20*) also failed to accumulate hyperphosphorylated forms of Kin4 in the absence of *LTE1* (Fig. 6 C).

The kinase Elm1 phosphorylates Kin4 at threonine 209 (T209) within its activation loop (Caydası et al., 2010b). Kin4-T209 phosphorylation is essential to promote Kin4 catalytic activity and appearance of the hyperphosphorylated forms of Kin4 whose migration is retarded on SDS-PAGE gels (Caydası et al., 2010b; Moore et al., 2010). We established that lack of Kin4 hyperphosphorylation was not due to inappropriate phosphorylation of Kin4 by Elm1 within the activation loop, as the levels of T209 phosphorylation were comparable to wild-type and *lte1* Δ cells (Fig. 6, D and E). Thus, Lte1 promotes hyperphosphorylation of active Kin4 *in vivo*.

The PP2A phosphatase subunit, Rts1, is important for the dephosphorylation and localization of Kin4. In *rts1* Δ cells, hyperphosphorylated Kin4, while retaining kinase activity, is unable to function in SPOC signaling with Bfa1. This is most likely due to its inability to bind to SPBs (Chan and Amon, 2009; Caydası et al., 2010b). We therefore asked whether hypophosphorylation of Kin4 in *lte1* Δ cells arose as a consequence of an influence over the function of PP2A-Rts1. If this were the case, deletion of *RTS1*

Figure 5. Functional relationship between Kin4 and Lte1 during normal cell cycle progression. (A) *lte1Δ* cells become more sensitive to increasing *KIN4* levels. The indicated strains carrying *LTE1* on a *URA3*-based plasmid were transformed with *KIN4* on a *LEU2*-based centromeric (*CEN-KIN4*) or 2 μ -based plasmid (2 μ -*KIN4*). Shown is the growth (2 d at 30°C) of serial dilutions of cells. (B) The indicated strains were arrested in G1 with α -factor in galactose-containing medium at 30°C. Cells were washed with glucose-containing medium to remove α -factor ($t = 0$) and to simultaneously induce UPL-Tem1 degradation. Bfa1-3HA, Clb2, and Upl-Tem1 were detected using anti-HA, anti-Clb2, and anti-Tem1 antibodies, respectively. Asterisks indicate Bfa1-3HA hyperphosphorylation forms. “C” is a control sample containing hyperphosphorylated Bfa1-3HA (enriched from *cdc15-1* cells arrested in late anaphase; Pereira and Schiebel, 2005). Tubulin served as loading control. (C) Indicated strains carrying *BFA1-3HA* were arrested with α -factor and released in α -factor-free medium. Samples of the indicated time points were run side by side for comparison of Bfa1 phosphorylation (see Fig. S4, C–F, for complete samples). The asterisk indicates Cdc5-dependent hyperphosphorylated Bfa1 form.



in *lte1Δ* cells should restore Kin4 hyperphosphorylation. Whereas Kin4-6HA was mainly hypophosphorylated in *lte1Δ* cells, phosphorylation of Kin4-6HA increased slightly in *lte1Δ rts1Δ* cells (Fig. 6 F). Re-introduction of *LTE1* in the *lte1Δ rts1Δ* background restored the full accumulation of hyperphosphorylated Kin4 (Fig. 6 F). Thus, the mechanism by which Lte1 promotes Kin4 phosphorylation is in part counteracted by PP2A-Rts1.

The hyperphosphorylated Kin4 species that arise in the absence of *RTS1* fail to bind to the mother cell cortex and the

SPB (Chan and Amon, 2009; Caydas et al., 2010b). To explore whether this was also the case in *lte1Δ rts1Δ* cells, we analyzed the localization of Kin4-GFP in cells carrying the SPB marker Spc42 fused to the red fluorescent protein eqFP611 (Spc42-eqFP; Wiedenmann et al., 2002). Cells were treated with nocodazole to increase the proportion of Kin4 associated with the SPB (Pereira and Schiebel, 2005). Kin4-GFP localized at the mother cell cortex and SPBs in both wild-type and *lte1Δ* cells (Fig. 6, G and H). In agreement with previous

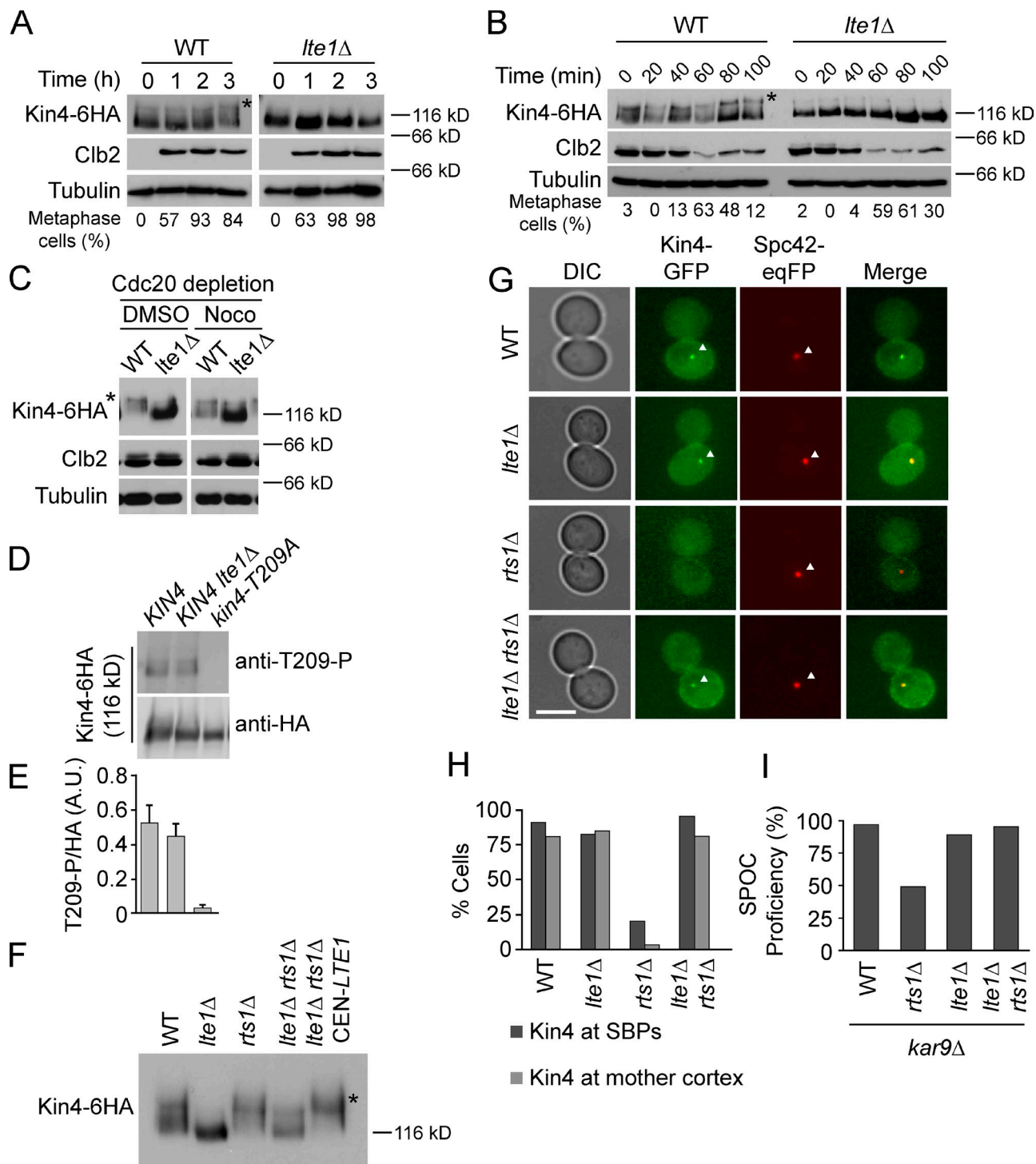


Figure 6. *Lte1* regulates the phosphorylation status of Kin4. (A and B) Phosphorylation of Kin4-6HA in the presence or absence of *LTE1*. (A) Cells carrying *KIN4-6HA* were synchronized in G1 with α -factor ($t = 0$) and released into media containing nocodazole to induce metaphase arrest and Kin4 phosphorylation (asterisk). (B) Nocodazole-arrested cells were released in nocodazole-free medium. Clb2 levels and percentage of metaphase cells were monitored over time. (C) Kin4-6HA of wild-type and *lte1* Δ cells arrested in metaphase upon *CDC20* depletion in the presence of solvent control (DMSO) or nocodazole. Asterisks mark Kin4-phosphorylated forms. Tubulin in A–C served as loading control. (D) *KIN4-6HA*, *KIN4-6HA lte1* Δ , and *kin4-T209A-6HA* strains, arrested in metaphase (*CDC20* depletion), were subjected to immunoprecipitation using anti-HA antibodies. The levels of Kin4-6HA and phosphorylation at T209 are shown. (E) Quantification of D. (F) Strains expressing *KIN4-6HA* were arrested in G1 with α -factor and released into medium containing nocodazole for 2 h at 30°C. CEN-*LTE1* indicates a centromeric plasmid carrying *LTE1*. Asterisk points to the Kin4-6HA-hyperphosphorylated form. (G) Kin4-GFP localization was determined by fluorescence microscopy in nocodazole-treated metaphase-arrested cells. Spc42-eqFP served as SPB marker (arrowheads). Bar, 5 μ m. (H) Quantification of G. (I) SPOC proficiency of the indicated strains grown at 23°C and shifted to 30°C for 4 h before inspection. G and I show one representative experiment of three. 100–150 cells were scored per sample.

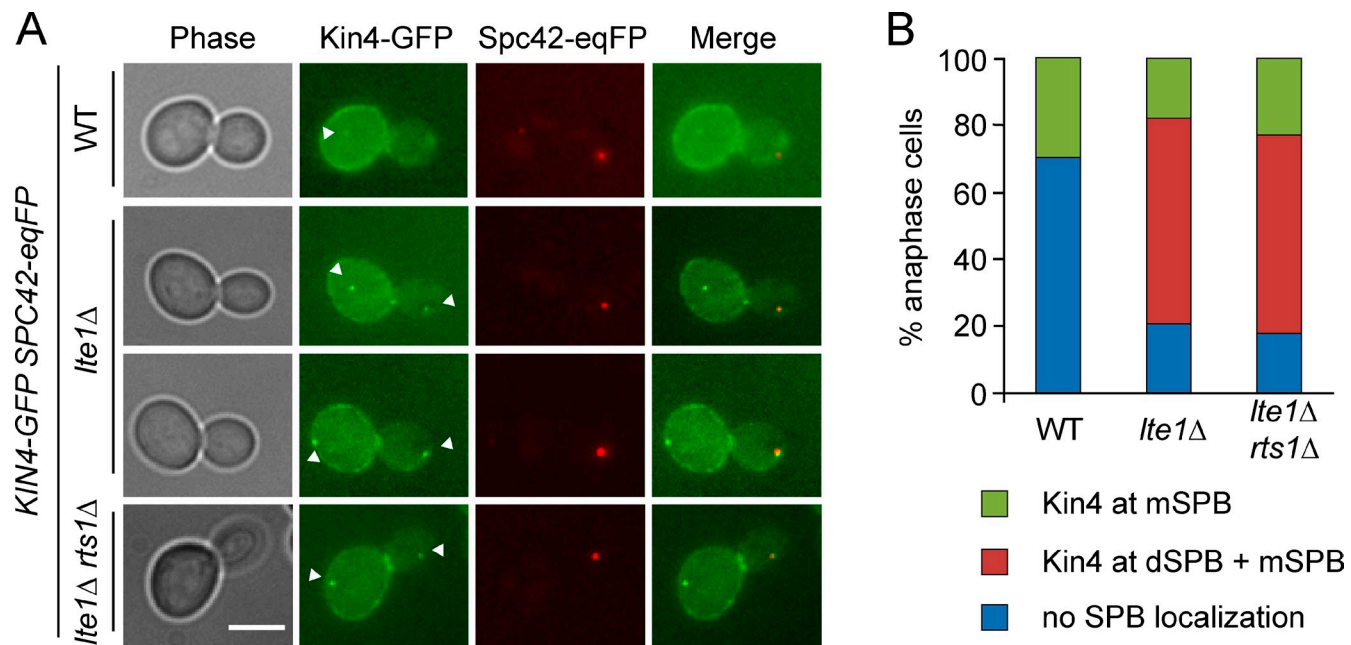


Figure 7. Lte1 regulates loading of Kin4 onto the dSPB. (A) Localization of Kin4-GFP monitored by fluorescence microscopy using unfixed cells. Spc42-eqFP served as SPB marker (arrowhead). Note that the SPB retained in the mother cell (new SPB) is weakly labeled due to the slow maturation property of Spc42-eqFP (Pereira et al., 2001). Bar, 5 μ m. (B) Quantification of A; 100–150 cells were scored per strain. One representative experiment of three is shown.

reports (Chan and Amon, 2009; Caydası et al., 2010b), deletion of *RTS1* resulted in the loss of the majority of the Kin4-GFP signal from both the cortex and the SPBs (Fig. 6, G and H). Interestingly, delocalization of Kin4 did not occur in *lte1* Δ *rts1* Δ cells (Fig. 6, G and H). This suggested that Kin4 escapes the control of PP2A-Rts1 in the absence of *LTE1*. In line with this hypothesis, deletion of *LTE1* rescued the SPOC deficiency of *kar9* Δ *rts1* Δ cells (Fig. 6 I). In conclusion, the data imply Lte1 and PP2A-Rts1 as having opposing impacts upon Kin4 phosphorylation and localization.

Lte1 inhibits the binding of Kin4 to the dSPB in anaphase

To further explore the role of Lte1 in regulating Kin4, we asked whether Lte1 would influence Kin4 localization in an unperturbed cell cycle (Fig. 7). In *LTE1* wild-type cells, Kin4 localizes preferentially at the mother cell cortex and from mid- to late anaphase onwards to the mSPB. Kin4-GFP was barely detected at the dSPB (Pereira and Schiebel, 2005). Deletion of *LTE1* profoundly affected localization of Kin4. In 5–7% of *lte1* Δ cells in anaphase, enhanced binding of Kin4-GFP to the daughter cell cortex was observed in comparison to 1–2% in *LTE1* wild-type cells (Fig. 7 A, *lte1* Δ , bottom panel; and unpublished data). The number of *lte1* Δ cells in which a Kin4-GFP signal could be detected at the dSPB during anaphase was greatly increased compared with wild-type cells at 30°C (Fig. 7, A and B; from <1% in *LTE1* to 62% in *lte1* Δ cells). This was even more pronounced at 14°C (<1% in *LTE1* in comparison to 80% in *lte1* Δ cells). Thus, Lte1 impinges upon the recruitment of Kin4 to the dSPB.

Interaction between Kin4 and Lte1 requires Cla4

The Pak kinase Cla4 contributes to mitotic exit by phosphorylating Lte1 and promoting Lte1's localization at the bud cell cortex (Höfken and Schiebel, 2002; Jensen et al., 2002; Seshan et al., 2002; Yoshida et al., 2003). In the absence of *CLA4*, Lte1 is no longer able to promote mitotic exit, showing that Cla4-dependent phosphorylation of Lte1 is essential for its mitotic function (Höfken and Schiebel, 2002; Seshan et al., 2002; Yoshida et al., 2003; Nelson and Cooper, 2007). Furthermore, we found that the growth defect of *cla4* Δ cells at lower temperatures (Höfken and Schiebel, 2002) was rescued by deletion of *KIN4* (Fig. 8 A), suggesting that increased Kin4 activity might contribute to the growth defect of *cla4* Δ cells. We therefore asked whether Cla4 influenced the ability of Lte1 to interact with Kin4. In *cla4* Δ cells, less Kin4 immunoprecipitated with Lte1 (Fig. 8, B and C), although the specific Kin4 catalytic activity, which is required for Lte1–Kin4 association (Fig. 3), was comparable to control cells (Fig. S3 D). Thus, Cla4 regulates Lte1–Kin4 complex formation.

Considering that mother cell–located Lte1 promotes mitotic exit of cells with misaligned spindles, we asked whether Lte1-GFP caused SPOC deficiency in *SFK1-GBP* *kar9* Δ cells in a Cla4-dependent manner. The binding of Lte1-GFP to Sfk1-GBP was Cla4 independent (Fig. 8 D). However, the bud cortex signal of Cla4-3Cherry was decreased in *LTE1-GFP SFK1-GBP* cells (unpublished data) and the phosphorylated forms of Lte1, which are observed in *SFK1-GBP* cells, were lost upon deletion of *CLA4* (Fig. 8 E). This suggested that Cla4-dependent Lte1 phosphorylation, which activates the mitotic function of Lte1, is in place in *SFK1-GBP* cells. In agreement with this

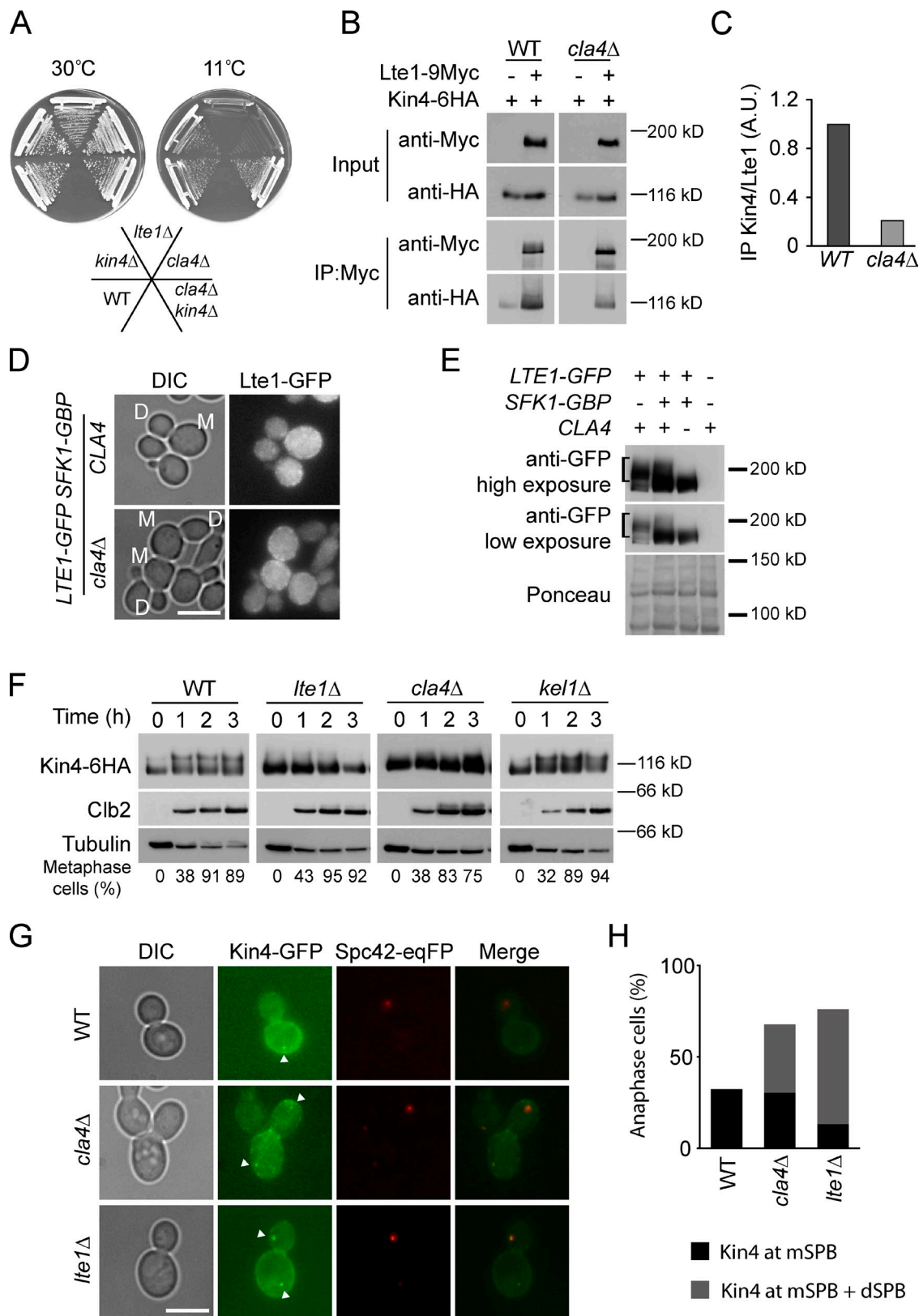


Figure 8. *Lte1*–*Kin4* interaction requires *Cla4*. (A) Growth of the indicated strains in YPD plates for 2 d (30°C) and 14 d (11°C). (B) Interaction between *Lte1*-9Myc and *Kin4*-6HA was investigated in wild-type (WT) and *cla4Δ* cells upon immunoprecipitation of *Lte1*-9Myc with anti-Myc beads. Note that this experiment was done with the experiment shown in Fig. 3 C; i.e., the blots of the WT strain are identical. (C) Quantification of B. One representative experiment of two is shown. (D) Localization of *Lte1*-GFP. (E) Phosphorylation profile of *Lte1*-GFP in the indicated strains. The brackets indicate *Lte1*-phosphorylated forms. (F) Strains were arrested with α -factor and released into nocodazole-containing media. *Kin4*-6HA and *Clb2* levels were determined by immunoblotting at the indicated time points. *Tubulin* served as a loading control. (G) Localization of *Kin4*-GFP. *Spc42*-eqFP served as SPB marker. (H) Quantification of G. One representative experiment of three is shown. Bar, 5 μ m.

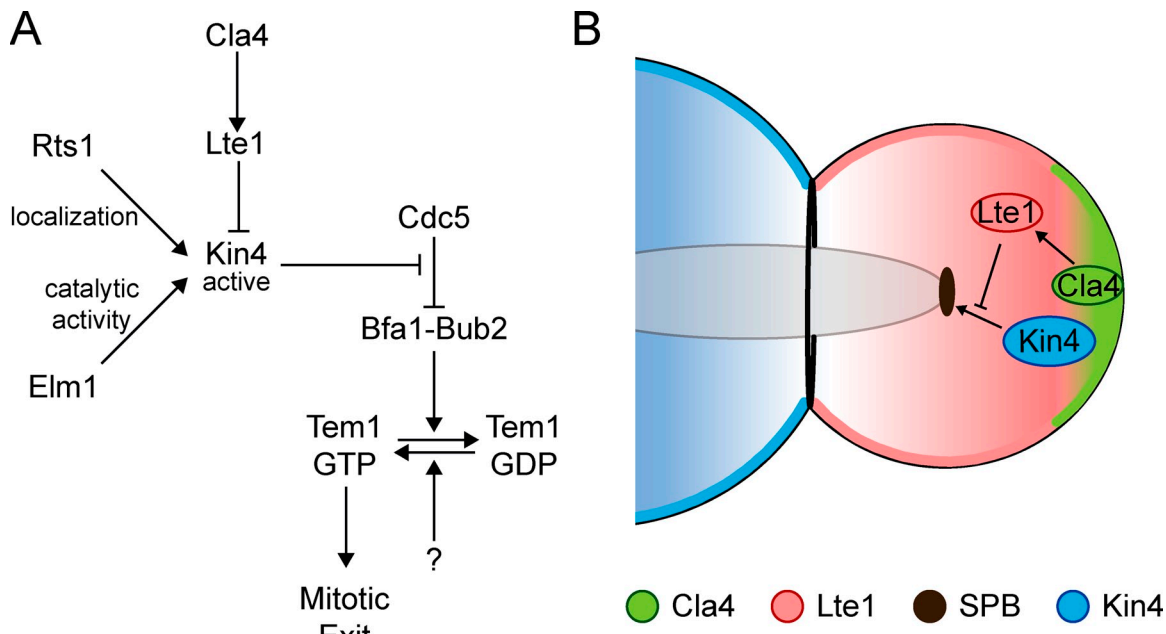


Figure 9. Model for Lte1 regulation of mitotic exit. (A) Lte1 functions upstream of Tem1 to promote mitotic exit. Both Elm1 and Rts1 control Kin4 activity by promoting Kin4 catalytic activity and localization, respectively. In contrast, Lte1 inhibits Kin4 catalytic activity, working upstream of Tem1. The kinase Cla4 is required for Lte1 to interact with Kin4. (B) Spatial regulation of Kin4 by Lte1. Cla4 activates Lte1 to inhibit the binding of Kin4 at dSPB to facilitate mitotic exit. See Discussion for details.

notion, the SPOC deficiency of *SFK1-GBP LTE1-GFP kar9Δ* cells was rescued by deletion of *CLA4* (unpublished data), which is in line with similar observations showing that deletion of *CLA4* rescues the SPOC deficiency of mother cell-enriched Lte1 (Nelson and Cooper, 2007).

If Lte1 regulates Kin4 in a Cla4-dependent manner, one would expect Kin4 phosphorylation and localization to be affected by deletion of *CLA4*. Indeed, similarly to *lte1Δ* strains, Kin4-hypophosphorylated forms accumulated in *cla4Δ* cells (Fig. 8 F). The reduction of Kin4 phosphorylation was specific to *CLA4* deletion, as Kin4 became hyperphosphorylated in *kel1Δ* cells in which Lte1 is phosphorylated but de-localized from the bud cortex (Fig. 8 F) (Höfken and Schiebel, 2002; Jensen et al., 2002; Seshan et al., 2002). In addition, Kin4-GFP also accumulated at the dSPB in *cla4Δ* cells (Fig. 8, G and H). However, in comparison to *lte1Δ*, dimmer SPB and more dispersed cytoplasmic Kin4-GFP signals were observed, most likely due to morphological defects caused by lack of Cla4 (unpublished data; Höfken and Schiebel, 2002). Together, these data strongly indicate that Cla4 is required by Lte1 to interact with and control Kin4 phosphorylation and localization.

Discussion

Since its discovery, Lte1 has been classified as a putative GEF for the MEN GTPase Tem1 (Shirayama et al., 1994a,b). Undoubtedly, Lte1 is an activator of mitotic exit; however, the mechanism by which it does so remains debatable. Our data now support a role for Lte1 in promoting mitotic exit by restraining the activity of the SPOC kinase Kin4. Lte1 and Kin4 physically interacted in vitro and were present in common complexes in vivo. In addition, Lte1 inhibited Kin4 catalytic activity

toward Bfa1 in vivo and in vitro. We propose that Lte1 contributes to mitotic exit working upstream of Tem1 through its inhibitory influence on the activity of Kin4 kinase (Fig. 9).

Requirements for Lte1-Kin4 interaction

Our data show that the in vivo interaction between Kin4 and Lte1 requires Kin4 kinase activity and the Pak kinase Cla4, but not the PP2A subunit Rts1. The requirement of Cla4 is explained by the regulation of Lte1 by Cla4. Only Lte1 that is phosphorylated by Cla4 is correctly localized to the bud cortex and has the ability to promote mitotic exit (Höfken and Schiebel, 2002; Jensen et al., 2002; Seshan et al., 2002; Yoshida et al., 2003; Nelson and Cooper, 2007). The kinase-dependent interaction between Kin4 and Lte1 is much less understood. Kin4 could phosphorylate Lte1 and thereby create a binding site for Kin4. However, there is presently no evidence supporting a role for Kin4 in phosphorylating Lte1. However, the phosphorylation profile of Lte1 is complex, as Cdk1, Cla4, and probably other kinases phosphorylate it in a cell cycle-dependent manner (Höfken and Schiebel, 2002; Jensen et al., 2002; Seshan et al., 2002). Thus, we cannot completely rule out the possibility that Kin4 phosphorylates sites in Lte1 and thereby creates a high-affinity binding site for itself. Alternatively, Kin4 catalytic activity might be required to dislodge a protein that inhibits Lte1-Kin4 complex formation. Detailed biochemical and biophysical analysis using purified components will be necessary to clarify the molecular requirements of Kin4 activity for the Kin4-Lte1 interaction.

Lte1-dependent Kin4 regulation

Our in vitro and in vivo studies suggested that Lte1 is an inhibitor of Kin4 catalytic activity. However, whereas in vitro analysis suggested that Lte1 might work as a competitive inhibitor of

Kin4 catalytic activity, analysis of Kin4 behavior in *lte1* Δ cells showed that the *in vivo* situation is more complex. Deletion of *LTE1* had a striking influence upon Kin4 phosphorylation. Interestingly, deletion of *LTE1* inhibited the appearance of hyperphosphorylated forms of Kin4; however, the activating phosphorylation of Kin4 at T209 by Elm1 was as in wild-type cells. Lte1 might control Kin4 by restricting the activity of a phosphatase or by acting as an adapter protein for a kinase that preferentially facilitates the hyperphosphorylation of catalytically active Kin4.

The phosphatase PP2A-Rts1 is involved in Kin4 dephosphorylation (Chan and Amon, 2009). The fact that deletion of *RTS1* only partially restored Kin4 hyperphosphorylation in the *lte1* Δ background implies that Lte1 might promote Kin4 hyperphosphorylation by activating a kinase rather than simply restricting PP2A-Rts1 activity over Kin4.

In addition to influencing Kin4's phosphorylation, Lte1 also affects Kin4 localization (Fig. 9). In the absence of Lte1, Kin4 accumulated at the dSPB in anaphase. This accumulation contrasts the wild-type situation, in which Kin4 is excluded from the daughter cell compartment. We therefore suggest that Lte1 makes a partial but important contribution to Kin4 asymmetry by excluding it from binding to the dSPB. At present, the relationship between Kin4 function, phosphorylation, and localization is not fully understood. Rts1 is crucial for the proper localization of Kin4 to the mother cortex and SPBs (Chan and Amon, 2009). Deletion of *RTS1* leads to the accumulation of hyperphosphorylated and mislocalized, catalytically active Kin4 species (Chan and Amon, 2009; Caydası et al., 2010b). Given that Kin4 needs to bind to SPBs to phosphorylate Bfa1 upon SPOC activation (Maekawa et al., 2007), the current understanding is that an Rts1-dependent dephosphorylation of Kin4 is required for Kin4 SPB association and hence SPOC function (Caydası and Pereira, 2009; Caydası et al., 2010b). Deletion of *LTE1* rescued Kin4 SPB localization in the *rts1* Δ background, despite the fact that Kin4 was partially hyperphosphorylated. The phosphorylation profile of Kin4 in *rts1* Δ and *rts1* Δ *lte1* Δ cells might differ in key amino acid residues.

How would deletion of *LTE1* restore Kin4 localization at mother and daughter SPBs in *rts1* Δ cells? One possibility is that Kin4 is locked in an intermediate phosphorylated state in *lte1* Δ cells, rendering it insensitive to PP2A-Rts1 control over Kin4 localization. Alternatively, Rts1 might regulate Kin4 localization working upstream of Lte1. In this respect, deletion of *LTE1* not only rescues the localization but also the SPOC deficiency of *rts1* Δ cells. This functional link might indicate that Rts1 could restrict the activity of Lte1 over Kin4; an exciting possibility that awaits detailed analysis. Interestingly, a cross talk between the fission yeast homologue of Lte1, Etd1, and the B-type regulatory phosphatase subunit of PP2A, Pab1, was recently described (García-Cortés and McCollum, 2009; Lahoz et al., 2010). A functional homologue of Kin4 in fission yeast has however not yet been identified.

Coordination of mitotic exit and SPOC by Lte1

Our data are consistent with the compartmentalization model that was proposed based on cellular phenotypes upon mislocalization

of Kin4 and Lte1 (Bardin et al., 2000; Castillon et al., 2003; D'Aquino et al., 2005; Maekawa et al., 2007; Geymonat et al., 2009a; Chan and Amon, 2010). Keeping Lte1 in the daughter cell is essential for SPOC function, whereas restricting Kin4 activity to the mother cell compartment is important for mitotic exit. We now provide a molecular understanding for the differential distribution of the Kin4 and Lte1 to mother and daughter cell compartments. Lte1 contributes to the exclusion of Kin4 from the dSPB in anaphase, which allows accumulation of Bub2–Bfa1 at the dSPB and subsequent Cdc5-dependent inactivation of the Bub2–Bfa1 GAP complex (Hu et al., 2001; Geymonat et al., 2003). This function of Lte1 is important during an unperturbed cell cycle most likely to inactivate any Kin4 that accidentally enters the daughter cell compartment.

It is however puzzling that deletion of *LTE1* also influenced the phosphorylation status of Kin4 in metaphase and upon SPOC activation, two conditions in which Lte1 and Kin4 should be confined to different cellular compartments. A fraction of Lte1 and Kin4 might however colocalize throughout the cell cycle, as supported by the fluorescent profiles of strains carrying Kin4-GFP and Lte1-3Cherry (Fig. 3). It is thus feasible that compartment-specific regulation of Lte1–Kin4 complexes might represent an important level of mitotic regulation, in addition to the control of Lte1 and Kin4 localization.

Previous reports established that forcing Kin4 onto the dSPB delayed mitotic exit and increased the symmetric binding of Bfa1 to SPBs in cells with normally aligned spindles (Maekawa et al., 2007; Caydası and Pereira, 2009; Geymonat et al., 2009a; Chan and Amon, 2010). At present it is unclear whether the delay in mitotic exit observed in *lte1* Δ at lower temperatures, which can be rescued by deletion of *BFA1* or *KIN4*, arises from the persistent binding of Kin4 to the dSPBs of anaphase cells. Nevertheless, recruitment of Kin4 to the dSPB would explain the increased symmetric localization of Bfa1 observed in *lte1* Δ cells (Geymonat et al., 2009a); a consequence of the increased Bfa1 dynamics in response to Kin4 activity at SPBs (Caydası and Pereira, 2009).

Cell polarity proteins function in parallel to Lte1 to promote mitotic exit (Höfken and Schiebel, 2002; Seshan et al., 2002; Chirolí et al., 2003). The Cdc42 effectors Gic1 and Gic2 were shown to contribute to mitotic exit (Höfken and Schiebel, 2004), possibly by inhibiting the activity of the Bub2–Bfa1 GAP complex. Lte1 and cell polarity determinants all localize to the bud tip, the site where microtubules are anchored by the dynein-dependent pathway (Yeh et al., 1995; Carminati and Stearns, 1997). Interestingly, Kar9 and the cyclin Clb4, which are proteins involved in cytoplasmic microtubule interaction with the cell cortex (Miller and Rose, 1998; Liakopoulos et al., 2003; Maekawa et al., 2003; Maekawa and Schiebel, 2004), also prevent binding of Kin4 to the dSPB by an unknown mechanism (Chan and Amon, 2010). It is thus tempting to speculate that proper cytoplasmic microtubule attachment negatively regulates Kin4 activity via Lte1 at the dSPB and/or alternative mechanisms to allow mitotic exit. This would be in line with a function for the SPBs as a sensor for spindle alignment, as previously suggested (Bardin et al., 2000; Gruneberg et al., 2000; Pereira et al., 2001; D'Aquino et al., 2005; Maekawa et al., 2007; Chan and Amon, 2010).

Centrosomes of higher eukaryotic cells play an important role in the orientation of the mitotic spindle in respect to the cell polarity axis, which is particularly important in cells undergoing asymmetric divisions (Yamashita and Fuller, 2008; Siller and Doe, 2009). It will be interesting to determine whether centrosomes also function as sensors to control cell cycle progression in respect to the cell polarity axis among eukaryotes, as recently suggested for *Drosophila* germ line stem cells (Cheng et al., 2008; Inaba et al., 2010).

Materials and methods

Growth conditions

Yeast growth conditions in solid and liquid media were as described previously (Sherman, 1991). Yeast strains were grown in yeast peptone dextrose medium with 0.1 mg/l adenine (YPAD). Temperature-sensitive strains were grown at 23°C and shifted to 37°C for phenotypic analysis. For live-cell imaging, yeast cultures were grown in filter-sterilized YPDA. Yeast peptone medium containing adenine and 3% raffinose (YPAR) was used to grow strains carrying genes under the Gal1 promoter (Gal1 promoter repressed). For induction of genes under the Gal1 promoter, galactose (2%) was added to cells growing in YPAR media.

Yeast strains and plasmids

Yeast strains and plasmids are listed in Table S1. Gene deletions and epitope tagging were performed using PCR-based methods (Knop et al., 1999; Janke et al., 2004). Gal1-CDC20 (Pereira and Schiebel, 2005), Gal1-Clb2ΔDB (Surana et al., 1993), and Gal1-UPL-TEM1 (Shou et al., 1999) were constructed using integration plasmids. All strains harboring a KAR9 deletion were maintained with KAR9 on a centromeric URA3-based plasmid and analyzed for phenotypes shortly after inducing plasmid loss on 5-fluoroorotic acid (5-FOA) containing plates. The GBP-KanMX4 cassette was constructed by replacing GFP from pYM12 (Knop et al., 1999) by the gene coding sequence of the GFP-binding protein (provided by Heinrich Leonhardt, Ludwig-Maximilians University, Munich, Germany).

Cell cycle analysis

For synchronization, yeast cells were incubated with 10 µg/ml α-factor (Sigma-Aldrich) for 2–2.5 h at 30°C until >95% of cells showed a mating projection. To arrest the cells with nocodazole, 15 µg/ml nocodazole (Sigma-Aldrich) was added to the culture media and incubated for 2–3 h. S-phase arrest was induced by adding 200 µM hydroxyurea (Sigma-Aldrich) to log phase cultures and further incubated for 2–3 h. To induce metaphase arrest of Gal1-CDC20 cells, cells grown in YPAR media containing 2% galactose were washed in YPAR media lacking galactose and further incubated in this media until >95% of the cells were large budded with one DAPI-staining region. Gal1-CDC20 cells, arrested in metaphase, were released from the cell cycle block by addition of 2% galactose.

Protein methods and reagents

Yeast protein extracts and immunoblotting were performed as described previously (Janke et al., 2004). In brief, cell pellets were collected by centrifugation and resuspended in 1 ml TCA-solution (7.5% trichloroacetic acid and 250 mM NaOH) and kept on ice for 15 min. Samples were centrifuged at 10,000 g for 20 min at 4°C. Precipitated proteins were resuspended in HU-DTT (200 mM Tris-HCl, pH 6.8, 8 M urea, 5% SDS, 0.1 mM EDTA, 0.005% Bromophenol blue, and 15 mg/ml DTT). Samples were heated up for 15 min at 65°C before loading onto SDS-PAGE gels. Coomassie Brilliant Blue G-250 (Invitrogen) was used to stain protein gels. For immunoblotting, proteins were transferred from SDS-PAGE gels onto nitrocellulose membrane and stained with Ponceau S (Sigma-Aldrich) before immunodetection was performed. The antibodies used were rabbit anti-GFP, rabbit anti-Tem1, mouse anti-GST (gift from Elmar Schiebel, University of Heidelberg, Heidelberg, Germany), mouse anti-HA (clone 12CA5; Sigma-Aldrich), mouse anti-Myc (clone 9E10; Sigma-Aldrich), rabbit anti-Clb2 and guinea-pig anti-Sic1 (Maekawa et al., 2007), mouse anti-tubulin (TAT1; Sigma-Aldrich), and mouse anti-His (GE Healthcare). Secondary antibodies were goat anti-mouse, goat anti-rabbit and goat anti-guinea pig IgGs coupled to horseradish peroxidase (Jackson ImmunoResearch Laboratories, Inc.).

Purification of Kin4 and Lte1 complexes

For the tandem affinity purifications (Puig et al., 2001), whole-cell extracts were prepared from 2 liters of exponentially growing yeast cells expressing KIN4-TAP or LTE1-TAP. Untagged, wild-type strains were used as a negative control. Cell pellets were lysed using acid-washed glass beads (Sigma-Aldrich). Lysates were cleared by centrifugation at 10,000 g for 20 min at 4°C and incubated with Magnetic beads coupled to IgGs (Dynabeads; Invitrogen). Immunoprecipitates were extensively washed with TAP buffer (50 mM Tris-HCl, pH 7.4, 1 mM EDTA, 10 mM DTT, 10% glycerol, and 400 mM NaCl). Kin4- and Lte1-interacting proteins were eluted with 0.5 N NH₄OH, 0.5 mM EDTA solution and identified by mass spectrometry (MS) upon digestion with trypsin.

Immunoprecipitation of proteins

Cell extracts were prepared from 250-ml (10⁷ cells/ml) yeast cultures. The cells were lysed using acid-washed glass beads (Sigma-Aldrich). The lysis buffer contained 50 mM Tris-HCl, pH 7.4, 250 mM NaCl, 10% glycerol, 10 mM EDTA, 1 mM DTT, 100 mM β-glycerophosphate, 50 mM NaF, 5 mM NaVO₃, and complete EDTA-free protease inhibitor cocktail (Roche). Cell lysates were incubated with 0.5% Triton X-100 for 10 min and total extract was clarified by centrifugation at 10,000 g for 15 min at 4°C. Proteins were immunoprecipitated with anti-HA or anti-Myc antibodies coupled to protein G-Sepharose (Invitrogen). Samples were boiled for 15 min in HU-DTT buffer before loading onto SDS-PAGE gels (Janke et al., 2004).

Recombinant protein purifications

6His-Lte1-N and 6His-Lte1-C were expressed in *E. coli* BL21 (DE3) using 0.1 mM IPTG. Fusion proteins were purified using Ni-NTA Agarose beads following the manufacturer's instructions (QIAGEN). Buffer exchange of 6His-fusion proteins after purification was performed using PD MiniTrap G-25 Sephadex columns (GE Healthcare). Bacterially expressed GST and GST-Kin4 were purified using glutathione-Sepharose beads (GE Healthcare). Bacterially expressed MBP-Bfa1 was purified from *E. coli* Rosetta (DE3) cells, as described previously (Maekawa et al., 2007). In brief, cell pellets were resuspended in MBP-buffer (20 mM Tris-HCl, pH 7.4, 200 mM NaCl, 1 mM EDTA, 4 mM DTT, and 1 mM PMSF) and lysed by sonication. The lysate was clarified by centrifugation (10,000 g for 15 min at 4°C) and incubated with amylose resin (New England Biolabs, Inc.) for 4 h at 4°C. After washing with MBP-buffer lacking DTT, MBP-Bfa1 was eluted from the amylose resin using MBP buffer containing 10 mM maltose (Sigma-Aldrich). Recombinant proteins were stored at -80°C.

Kinase assays

For kinase reactions using yeast-enriched Kin4, Kin4-6HA was immunoprecipitated using protein G-Sepharose beads coupled to anti-HA antibodies. Kinase assays were performed in a kinase buffer containing 20 mM Hepes, pH 7.4, 0.5 mM EDTA, 5 mM MgCl₂, 0.5 mM DTT, 0.05 µM ATP, and 1 µg MBP-Bfa1 (Maekawa et al., 2007). 5 µCi γ-[³²P]ATP (0.05 nM) was used in each kinase reaction. The reactions were incubated for 30 min at 30°C.

For in vitro kinase reactions using purified GST-Kin4 from yeast, GST-Kin4 and GST-Kin4-T209A were purified from 2 liters of yeast cultures as described previously (Geymonat et al., 2009b). In brief, yeast cell pellets were resuspended in lysis buffer (50 mM Tris-HCl, pH 7.5, 250 mM NaCl, 5 mM EDTA, and 10% glycerol) containing 1% nonylphenyl-polyethylene glycol (NP-40) and protease inhibitors (Roche). Cells were lysed using acid-washed glass beads (Sigma-Aldrich). After centrifugation (10,000 g, 4°C, 20 min), the clarified cell extract was incubated with glutathione-Sepharose beads (GE Healthcare) for 2 h at 4°C. After extensive washings in lysis buffer, GST-Kin4 or GST-Kin4-T209A was eluted with 20 mM reduced glutathione (Sigma-Aldrich) in 50 mM Tris-HCl, pH 7.8, and 150 mM NaCl. Purified proteins were kept at -80°C.

For competition assays, GST-Kin4 (34 pmol per reaction) was incubated for 5 min at 30°C with recombinant 6His-GFP, 6His-Lte1-N, or 6His-Lte1-C, followed by addition of MBP-Bfa1 and 5 µCi γ-[³²P]ATP (0.05 nM) for 30 min at 30°C. Radioactivity was detected using the Bas 1800 II imaging system (Fujifilm). Quantifications of radioactive signals were performed using ImageJ Image processing and Analysis Software (National Institutes of Health, Bethesda, MD).

Fluorescence microscopy

Yeast cells harboring Kin4-GFP and Lte1-3Cherry were grown in YPDA or YPARGal plates and analyzed by fluorescence microscopy without washing or fixation. A Z-series of 0.3-µm steps were captured with a microscope (Axiovert 200M; Carl Zeiss) equipped with a 100x NA 1.45 Plan-Fluor oil immersion objective (Carl Zeiss), Cascade 1K CCD camera (Photometrics), and

MetaMorph software (Universal Imaging Corp.). The measurements of fluorescence intensities were made using sum-projected images and ImageJ software.

For budding index analysis, cells were fixed with 70% ethanol and resuspended in PBS containing 1 μ g/ml DAPI (Sigma-Aldrich). The distribution of DNA stained regions and the size of the buds were counted for 150–200 cells per time point.

Images were processed in ImageJ, Adobe Photoshop CS3, and Adobe Illustrator CS3. No manipulations were performed other than brightness, contrast, and color balance adjustments.

SPOC proficiency analysis

For determination of SPOC proficiency, *kar9Δ* cells carrying *TUB1-GFP* or *TUB1-3Cherry* were grown at 23°C and shifted to 30°C for 3 h. Cells were inspected after fixation with paraformaldehyde for 10 min at room temperature. DNA was stained with DAPI. SPOC proficiency was calculated by dividing the number of SPOC-arrested cells (cells containing two separated DAPI-stained regions and an intact anaphase spindle inside the mother cell) by the sum of SPOC-deficient and arrested cells (cells with more than two DAPI-stained regions in the mother cell body and broken and/or short spindles). 150–200 anaphase cells were counted per sample. Each experiment was done in triplicate.

Online supplemental material

Fig. S1 shows the Kin4 and Lte1 interactors identified by MS analysis and the coimmunoprecipitations using Kin4 and Lte1 as a bait. Fig. S2 shows the coimmunoprecipitation experiments using Lte1 or Kin4 as bait. Fig. S3 shows Kin4-specific kinase activity in wild-type and *lte1Δ* cells. Fig. S4 shows the Bfa1 phosphorylation profile in the absence or presence of Lte1. Table S1 presents the list of strains and plasmids used in this paper. Online supplemental material is available at <http://www.jcb.org/cgi/content/full/jcb.201101056/DC1>.

We acknowledge Elmar Schiebel and Heinrich Leonhardt for reagents and Ingrid Grummt for sharing equipment. We thank Thomas Ruppert for mass spectrometry analysis, Marcio Lazzarini for help with statistics, Ayse Caydası and Astrid Hofmann for technical support, and Elmar Schiebel, Iain Hagan, Fouzia Ahmad, and Ayse Caydası for helpful comments on this manuscript.

The Helmholtz association grant (HZ-NG-111) and Marie Curie fellowship (MEXT-CT-2006-042544) supported the work of G. Pereira; D.T. Bertazzi and B. Kurtulmus are Marie Curie fellows.

Submitted: 13 January 2011

Accepted: 16 May 2011

References

Adames, N.R., J.R. Oberle, and J.A. Cooper. 2001. The surveillance mechanism of the spindle position checkpoint in yeast. *J. Cell Biol.* 153:159–168. doi:10.1083/jcb.153.1.159

Audhya, A., and S.D. Emr. 2002. Stt4 PI 4-kinase localizes to the plasma membrane and functions in the Pkc1-mediated MAP kinase cascade. *Dev. Cell.* 2:593–605. doi:10.1016/S1534-5807(02)00168-5

Bardin, A.J., and A. Amon. 2001. Men and sin: what's the difference? *Nat. Rev. Mol. Cell Biol.* 2:815–826. doi:10.1038/35099020

Bardin, A.J., R. Visintin, and A. Amon. 2000. A mechanism for coupling exit from mitosis to partitioning of the nucleus. *Cell.* 102:21–31. doi:10.1016/S0092-8674(00)00007-6

Carminati, J.L., and T. Stearns. 1997. Microtubules orient the mitotic spindle in yeast through dynein-dependent interactions with the cell cortex. *J. Cell Biol.* 138:629–641. doi:10.1083/jcb.138.3.629

Castillon, G.A., N.R. Adames, C.H. Rosello, H.S. Seidel, M.S. Longtine, J.A. Cooper, and R.A. Heil-Chapdelaine. 2003. Septins have a dual role in controlling mitotic exit in budding yeast. *Curr. Biol.* 13:654–658. doi:10.1016/S0960-9822(03)00247-1

Caydası, A.K., and G. Pereira. 2009. Spindle alignment regulates the dynamic association of checkpoint proteins with yeast spindle pole bodies. *Dev. Cell.* 16:146–156. doi:10.1016/j.devcel.2008.10.013

Caydası, A.K., B. Ibrahim, and G. Pereira. 2010a. Monitoring spindle orientation: Spindle position checkpoint in charge. *Cell Div.* 5:28. doi:10.1186/1747-1028-5-28

Caydası, A.K., B. Kurtulmus, M.I.L. Orrico, A. Hofmann, B. Ibrahim, and G. Pereira. 2010b. Elm1 kinase activates the spindle position checkpoint kinase Kin4. *J. Cell Biol.* 190:975–989. doi:10.1083/jcb.201006151

Chan, L.Y., and A. Amon. 2009. The protein phosphatase 2A functions in the spindle position checkpoint by regulating the checkpoint kinase Kin4. *Genes Dev.* 23:1639–1649. doi:10.1101/gad.1804609

Chan, L.Y., and A. Amon. 2010. Spindle position is coordinated with cell-cycle progression through establishment of mitotic exit-activating and -inhibitory zones. *Mol. Cell.* 39:444–454. doi:10.1016/j.molcel.2010.07.032

Cheng, J., N. Turkel, N. Hemati, M.T. Fuller, A.J. Hunt, and Y.M. Yamashita. 2008. Centrosome misorientation reduces stem cell division during aging. *Nature.* 456:599–604. doi:10.1038/nature07386

Chirolı, E., R. Fraschini, A. Beretta, M. Tonelli, G. Lucchini, and S. Piatti. 2003. Budding yeast PAK kinases regulate mitotic exit by two different mechanisms. *J. Cell Biol.* 160:857–874. doi:10.1083/jcb.200209097

Christianson, T.W., R.S. Sikorski, M. Dante, J.H. Shero, and P. Hieter. 1992. Multifunctional yeast high-copy-number shuttle vectors. *Gene.* 110:119–122. doi:10.1016/0378-1119(92)90454-W

D'Aquino, K.E., F. Monje-Casas, J. Paulson, V. Reiser, G.M. Charles, L. Lai, K.M. Shokat, and A. Amon. 2005. The protein kinase Kin4 inhibits exit from mitosis in response to spindle position defects. *Mol. Cell.* 19:223–234. doi:10.1016/j.molcel.2005.06.005

Fraschini, R., M. Venturini, E. Chirolı, and S. Piatti. 2008. The spindle position checkpoint: how to deal with spindle misalignment during asymmetric cell division in budding yeast. *Biochem. Soc. Trans.* 36:416–420. doi:10.1042/BST0360416

García-Cortés, J.C., and D. McCollum. 2009. Proper timing of cytokinesis is regulated by *Schizosaccharomyces pombe* Etd1. *J. Cell Biol.* 186:739–753. doi:10.1083/jcb.200902116

Geymonat, M., A. Spanos, P.A. Walker, L.H. Johnston, and S.G. Sedgwick. 2003. In vitro regulation of budding yeast Bfa1/Bub2 GAP activity by Cdc5. *J. Biol. Chem.* 278:14591–14594. doi:10.1074/jbc.C300059200

Geymonat, M., A. Spanos, G. de Bettignies, and S.G. Sedgwick. 2009a. Lte1 contributes to Bfa1 localization rather than stimulating nucleotide exchange by Tem1. *J. Cell Biol.* 187:497–511. doi:10.1083/jcb.200905114

Geymonat, M., A. Spanos, and S. Sedgwick. 2009b. Production of mitotic regulators using an autoselection system for protein expression in budding yeast. *Methods Mol. Biol.* 545:63–80. doi:10.1007/978-1-60327-993-2_4

Gruneberg, U., K. Campbell, C. Simpson, J. Grindlay, and E. Schiebel. 2000. Nud1p links astral microtubule organization and the control of exit from mitosis. *EMBO J.* 19:6475–6488. doi:10.1093/emboj/19.23.6475

Höfken, T., and E. Schiebel. 2002. A role for cell polarity proteins in mitotic exit. *EMBO J.* 21:4851–4862. doi:10.1093/emboj/cdf481

Höfken, T., and E. Schiebel. 2004. Novel regulation of mitotic exit by the Cdc42 effectors Gic1 and Gic2. *J. Cell Biol.* 164:219–231. doi:10.1083/jcb.200309080

Hu, F., Y. Wang, D. Liu, Y. Li, J. Qin, and S.J. Elledge. 2001. Regulation of the Bub2/Bfa1 GAP complex by Cdc5 and cell cycle checkpoints. *Cell.* 107:655–665. doi:10.1016/S0092-8674(01)00580-3

Inaba, M., H. Yuan, V. Salzmann, M.T. Fuller, and Y.M. Yamashita. 2010. E-cadherin is required for centrosome and spindle orientation in *Drosophila* male germline stem cells. *PLoS ONE.* 5:e12473. doi:10.1371/journal.pone.0012473

Janke, C., M.M. Magiera, N. Rathfelder, C. Taxis, S. Reber, H. Maekawa, A. Moreno-Borchart, G. Doenges, E. Schwob, E. Schiebel, and M. Knop. 2004. A versatile toolbox for PCR-based tagging of yeast genes: new fluorescent proteins, more markers and promoter substitution cassettes. *Yeast.* 21:947–962. doi:10.1002/yea.1142

Jaspersen, S.L., and D.O. Morgan. 2000. Cdc14 activates cdc15 to promote mitotic exit in budding yeast. *Curr. Biol.* 10:615–618. doi:10.1016/S0960-9822(00)00491-7

Jensen, S., M. Geymonat, A.L. Johnson, M. Segal, and L.H. Johnston. 2002. Spatial regulation of the guanine nucleotide exchange factor Lte1 in *Saccharomyces cerevisiae*. *J. Cell Sci.* 115:4977–4991. doi:10.1242/jcs.00189

Keng, T., M.W. Clark, R.K. Storms, N. Fortin, W. Zhong, B.F. Ouellette, A.B. Barton, D.B. Kaback, and H. Bussey. 1994. LTE1 of *Saccharomyces cerevisiae* is a 1435 codon open reading frame that has sequence similarities to guanine nucleotide releasing factors. *Yeast.* 10:953–958. doi:10.1002/yea.320100710

Khmelinskii, A., J. Roostalu, H. Roque, C. Antony, and E. Schiebel. 2009. Phosphorylation-dependent protein interactions at the spindle midzone mediate cell cycle regulation of spindle elongation. *Dev. Cell.* 17:244–256. doi:10.1016/j.devcel.2009.06.011

Knop, M., K. Siegers, G. Pereira, W. Zachariae, B. Winsor, K. Nasmyth, and E. Schiebel. 1999. Epitope tagging of yeast genes using a PCR-based strategy: more tags and improved practical routines. *Yeast.* 15(10B):963–972. doi:10.1002/(SICI)1097-0061(199907)15:10B<963::AID-YEA399>3.0.CO;2-W

König, C., H. Maekawa, and E. Schiebel. 2010. Mutual regulation of cyclin-dependent kinase and the mitotic exit network. *J. Cell Biol.* 188:351–368. doi:10.1083/jcb.200911128

Lahoz, A., M. Alcaide-Gavilán, R.R. Daga, and J. Jimenez. 2010. Antagonistic roles of PP2A-Pab1 and Etd1 in the control of cytokinesis in fission yeast. *Genetics*. 186:1261–1270. doi:10.1534/genetics.110.121368

Liakopoulos, D., J. Kusch, S. Grava, J. Vogel, and Y. Barral. 2003. Asymmetric loading of Kar9 onto spindle poles and microtubules ensures proper spindle alignment. *Cell*. 112:561–574. doi:10.1016/S00092-8674(03)00119-3

Maeder, C.I., M.A. Hink, A. Kinkhabwala, R. Mayr, P.I. Bastiaens, and M. Knop. 2007. Spatial regulation of Fus3 MAP kinase activity through a reaction-diffusion mechanism in yeast pheromone signalling. *Nat. Cell Biol.* 9:1319–1326. doi:10.1038/ncb1652

Maekawa, H., and E. Schiebel. 2004. Cdk1-Clb4 controls the interaction of astral microtubule plus ends with subdomains of the daughter cell cortex. *Genes Dev.* 18:1709–1724. doi:10.1101/gad.298704

Maekawa, H., T. Usui, M. Knop, and E. Schiebel. 2003. Yeast Cdk1 translocates to the plus end of cytoplasmic microtubules to regulate bud cortex interactions. *EMBO J.* 22:438–449. doi:10.1093/emboj/cdg063

Maekawa, H., C. Priest, J. Lechner, G. Pereira, and E. Schiebel. 2007. The yeast centrosome translates the positional information of the anaphase spindle into a cell cycle signal. *J. Cell Biol.* 179:423–436. doi:10.1083/jcb.200705197

Miller, R.K., and M.D. Rose. 1998. Kar9p is a novel cortical protein required for cytoplasmic microtubule orientation in yeast. *J. Cell Biol.* 140:377–390. doi:10.1083/jcb.140.2.377

Moore, J.K., P. Chudalayandi, R.A. Heil-Chapdelaine, and J.A. Cooper. 2010. The spindle position checkpoint is coordinated by the Elm1 kinase. *J. Cell Biol.* 191:493–503. doi:10.1083/jcb.201006092

Nelson, S.A., and J.A. Cooper. 2007. A novel pathway that coordinates mitotic exit with spindle position. *Mol. Biol. Cell.* 18:3440–3450. doi:10.1091/mbc.E07-03-0242

Pereira, G., and E. Schiebel. 2005. Kin4 kinase delays mitotic exit in response to spindle alignment defects. *Mol. Cell.* 19:209–221. doi:10.1016/j.molcel.2005.05.030

Pereira, G., T. Höfken, J. Grindlay, C. Manson, and E. Schiebel. 2000. The Bub2p spindle checkpoint links nuclear migration with mitotic exit. *Mol. Cell.* 6:1–10.

Pereira, G., T.U. Tanaka, K. Nasmyth, and E. Schiebel. 2001. Modes of spindle pole body inheritance and segregation of the Bfa1p-Bub2p checkpoint protein complex. *EMBO J.* 20:6359–6370. doi:10.1093/embj/20.22.6359

Puig, O., F. Caspary, G. Rigaut, B. Rutz, E. Bouveret, E. Bragado-Nilsson, M. Wilm, and B. Séraphin. 2001. The tandem affinity purification (TAP) method: a general procedure of protein complex purification. *Methods*. 24:218–229. doi:10.1006/meth.2001.1183

Rothbauer, U., K. Zolghadr, S. Muyldermans, A. Schepers, M.C. Cardoso, and H. Leonhardt. 2008. A versatile nanotrap for biochemical and functional studies with fluorescent fusion proteins. *Mol. Cell. Proteomics*. 7:282–289.

Segal, M., and K. Bloom. 2001. Control of spindle polarity and orientation in *Saccharomyces cerevisiae*. *Trends Cell Biol.* 11:160–166. doi:10.1016/S0962-8924(01)01954-7

Seshan, A., A.J. Bardin, and A. Amon. 2002. Control of Lte1 localization by cell polarity determinants and Cdc14. *Curr. Biol.* 12:2098–2110. doi:10.1016/S0960-9822(02)01388-X

Sherman, F. 1991. Getting started with yeast. *Methods Enzymol.* 194:3–21. doi:10.1016/0076-6879(91)94004-V

Shirayama, M., Y. Matsui, K. Tanaka, and A. Toh-e. 1994a. Isolation of a CDC25 family gene, MSI2/LTE1, as a multicopy suppressor of ira1. *Yeast*. 10:451–461. doi:10.1002/yea.320100404

Shirayama, M., Y. Matsui, and A. Toh-e. 1994b. The yeast TEM1 gene, which encodes a GTP-binding protein, is involved in termination of M phase. *Mol. Cell. Biol.* 14:7476–7482.

Shou, W., J.H. Seol, A. Shevchenko, C. Baskerville, D. Moazed, Z.W. Chen, J. Jang, A. Shevchenko, H. Charbonneau, and R.J. Deshaies. 1999. Exit from mitosis is triggered by Tem1-dependent release of the protein phosphatase Cdc14 from nucleolar RENT complex. *Cell*. 97:233–244. doi:10.1016/S0092-8674(00)80733-3

Sikorski, R.S., and P. Hietter. 1989. A system of shuttle vectors and yeast host strains designed for efficient manipulation of DNA in *Saccharomyces cerevisiae*. *Genetics*. 122:19–27.

Siller, K.H., and C.Q. Doe. 2009. Spindle orientation during asymmetric cell division. *Nat. Cell Biol.* 11:365–374. doi:10.1038/ncb0409-365

Straight, A.F., W.F. Marshall, J.W. Sedat, and A.W. Murray. 1997. Mitosis in living budding yeast: anaphase A but no metaphase plate. *Science*. 277:574–578. doi:10.1126/science.277.5325.574

Surana, U., A. Amon, C. Dowzer, J. McGrew, B. Byers, and K. Nasmyth. 1993. Destruction of the CDC28/CLB mitotic kinase is not required for the metaphase to anaphase transition in budding yeast. *EMBO J.* 12:1969–1978.

Takizawa, P.A., J.L. DeRisi, J.E. Wilhelm, and R.D. Vale. 2000. Plasma membrane compartmentalization in yeast by messenger RNA transport and a septin diffusion barrier. *Science*. 290:341–344. doi:10.1126/science.290.5490.341

Wiedenmann, J., A. Schenk, C. Röcker, A. Girod, K.D. Spindler, and G.U. Nienhaus. 2002. A far-red fluorescent protein with fast maturation and reduced oligomerization tendency from *Entacmaea quadricolor* (Anthozoa, Actinaria). *Proc. Natl. Acad. Sci. USA*. 99:11646–11651. doi:10.1073/pnas.182157199

Yamashita, Y.M., and M.T. Fuller. 2008. Asymmetric centrosome behavior and the mechanisms of stem cell division. *J. Cell Biol.* 180:261–266. doi:10.1083/jcb.200707083

Yamashita, Y.M., A.P. Mahowald, J.R. Perlin, and M.T. Fuller. 2007. Asymmetric inheritance of mother versus daughter centrosome in stem cell division. *Science*. 315:518–521. doi:10.1126/science.1134910

Yeh, E., R.V. Skibbens, J.W. Cheng, E.D. Salmon, and K. Bloom. 1995. Spindle dynamics and cell cycle regulation of dynein in the budding yeast, *Saccharomyces cerevisiae*. *J. Cell Biol.* 130:687–700. doi:10.1083/jcb.130.3.687

Yoshida, S., R. Ichihashi, and A. Toh-e. 2003. Ras recruits mitotic exit regulator Lte1 to the bud cortex in budding yeast. *J. Cell Biol.* 161:889–897. doi:10.1083/jcb.200301128